PLOS PATHOGENS

A novel 4-aminoquinoline chemotype with multistage antimalarial activity and lack of cross-resistance with PfCRT and PfMDR1 mutants

Letícia Tiburcio Ferreira[1,2,3], Gustavo Capatti Cassiano[4], Luis Carlos Salazar Alvarez[1], John Okombo[2,3], Juliana Calit[5], Diana Fontinha[6], Eva Gil-Iturbe[7], Rachael Coyle[8,9], Carolina Horta Andrade[10,11,12], Per Sunnerhagen[13], Daniel Youssef Bargieri[5], Miguel Prudêncio[6], Matthias Quick[7,14,15], Pedro V. Cravo[4], Marcus C. S. Lee[8,9] David A. Fidock[2,3,16☯*], Fabio Trindade Maranhão Costa[1,4☯*]

1 Laboratory of Tropical Diseases-Prof. Dr. Luiz Jacintho da Silva, Department of Genetics, Evolution, Microbiology and Immunology, University of Campinas-UNICAMP, Campinas, São Paulo, Brazil, 2 Department of Microbiology and Immunology, Columbia University Irving Medical Center, New York, New York, United States of America, 3 Center for Malaria Therapeutics and Antimicrobial Resistance, Columbia University Irving Medical Center, New York, New York, United States of America, 4 Global Health and Tropical Medicine, Associate Laboratory in Translation and Innovation Towards Global Health, LA-REAL, Instituto de Higiene e Medicina Tropical, Universidade NOVA de Lisboa, Lisboa, Portugal, 5 Department of Parasitology, Institute of Biomedical Sciences, University of São Paulo, São Paulo, São Paulo, Brazil, 6 Instituto de Medicina Molecular João Lobo Antunes, Faculdade de Medicina da Universidade de Lisboa, Lisboa, Portugal, 7 Department of Psychiatry, Columbia University Irving Medical Center, New York, New York, United States of America, 8 Wellcome Sanger Institute, Wellcome Genome Campus, Hinxton, United Kingdom, 9 Biological Chemistry and Drug Discovery, Wellcome Centre for Anti-Infectives Research, University of Dundee, Dundee, United Kingdom, 10 Laboratory of Molecular Modeling and Drug Design, Faculty of Pharmacy, Universidade Federal de Goiás, Goiânia, Goiás, Brazil, 11 Center for the Research and Advancement in Fragments and molecular Targets, School of Pharmaceutical Sciences at Ribeirao Preto, University of São Paulo, Ribeirão Preto, São Paulo, Brazil, 12 Center for Excellence in Artificial Intelligence, Institute of Informatics, Universidade Federal de Goiás, Goiânia, Goiás, Brazil, 13 Department of Chemistry and Molecular Biology, University of Gothenburg, Gothenburg, Sweden, 14 Department of Physiology & Cellular Biophysics, Columbia University Irving Medical Center, New York, New York, United States of America, 15 New York State Psychiatric Institute, Area Neuroscience – Molecular Therapeutics, New York, New York, United States of America, 16 Division of Infectious Diseases, Columbia University Irving Medical Center, New York, New York, United States of America

☯ These authors contributed equally to this work.
* df2260@cumc.columbia.edu (DAF); fabiotmc72@gmail.com (FTMC)

Abstract

Artemisinin-based combination therapy (ACT) is the mainstay of effective treatment of *Plasmodium falciparum* malaria. However, the long-term utility of ACTs is imperiled by widespread partial artemisinin resistance in Southeast Asia and its recent emergence in parts of East Africa. This underscores the need to identify chemotypes with new modes of action (MoAs) to circumvent resistance to ACTs. In this study, we characterized the asexual blood stage antiplasmodial activity and resistance mechanisms of LDT-623, a 4-aminoquinoline (4-AQ). We also detected LDT-623 activity against multiple stages (liver schizonts, stage IV-V gametocytes, and ookinetes) of *Plasmodium*'s life cycle, a feature unlike other 4-AQs such as chloroquine (CQ) and piperaquine (PPQ). Using heme fractionation profiling and drug uptake studies in PfCRT-containing proteoliposomes, we observed inhibition of

hemozoin formation and PfCRT-mediated transport, which constitute characteristic features of 4-AQs' MoA. We also found minimal cross-resistance to LDT-623 in a panel of mutant *pfcrt* or *pfmdr1* lines, but not the PfCRT F145I mutant that is highly resistant to PPQ resistance yet is very unfit. No *P. falciparum* parasites were recovered in an *in vitro* resistance selection study, suggesting a high barrier for resistance to emerge. Finally, a competitive growth assay comprising >50 barcoded parasite lines with mutated resistance mediators or major drug targets found no evidence of cross-resistance. Our findings support further exploration of this promising 4-AQ.

Author summary

The emergence of artemisinin-resistant malaria parasites, first in Southeast Asia and more recently East Africa, highlights the urgency to identify and optimize chemotypes with antimalarial activity that are not compromised by known resistance mechanisms in clinical settings. Using a computer-aided drug discovery approach, we previously identified a 4-AQ (LDT-611) that was active against *P. falciparum* asexual blood-stage (ABS) parasites. Herein, we report the multistage antimalarial activity of a structural analog, a side-chain-modified 4-AQ (LDT-623). This analog shares 4-AQ characteristics, such as PfCRT-mediated transport, as well as inhibition of hemozoin formation, that occurs in the parasite digestive vacuole. Cross-resistance profiling showed that this compound was not compromised by known mutations in the digestive vacuole transporters PfCRT or PfMDR1 or by other gene products that govern resistance to antimalarials under development. Efforts to evolve resistance to LDT-623 *in vitro* yielded parasite populations lacking noticeable phenotypic changes. In conclusion, we report a 4-AQ whose MoA is likely to differ from licensed antimalarials within this chemical class, paving the way for further studies on this chemotype as a therapeutic avenue to treat multidrug-resistant malaria.

1. Introduction

Malaria remains a major global health concern, with the World Health Organization (WHO) reporting 249 million cases and 608,000 related deaths across 85 malaria-endemic countries and areas in 2022 [1]. Of the human-infecting *Plasmodium* species, *P. falciparum* is the most devastating due to its impact on mortality and morbidity, especially in young children and pregnant women. Currently, artemisinin (ART)-based combination therapies (ACTs) constitute the frontline antimalarial treatment policy [1]. ACTs comprise a rapid-acting yet short-lived ART derivative that eliminates most of the initial parasite load, partnered with a longer-lasting molecule with a distinct MoA to eliminate surviving parasites. The efficacy of ACTs has, however, been compromised by the emergence of mutant *k13* parasites in Southeast Asia [2–4] and parts of East Africa [5–7]. Parasites with specific *k13* mutations exhibit partial resistance to artemisinin, characterized by delayed clearance time upon treatment with an ART derivative or an ACT [8–10] and higher levels of ring-stage parasite survival *in vitro* [11]. This threat to the long-term therapeutic utility of ACTs calls for urgent efforts to identify and develop new molecules, preferably with divergent MoAs, no cross-resistance to existing molecules, and pan-activity across multiple stages of the *Plasmodium* lifecycle.

In the human host, the *P. falciparum* lifecycle involves the invasion of hepatocytes by sporozoites injected by a feeding female *Anopheles* mosquito. Liver-stage parasites mature and are

released into the bloodstream as merozoites that invade red blood cells (RBCs) to initiate the pathogenic asexual blood stage (ABS) cycle. This cycle lasts ~48 hours and is characterized by differentiation of the merozoites into ring forms then into trophozoites and ultimately schizonts, from which more merozoites egress and reinvade other RBCs. Some merozoites can also differentiate into sexual gametocyte forms that once mature can be transmitted to a feeding mosquito.

ABS parasites digest host hemoglobin (Hb) in their acidic digestive vacuole (DV), leading to the release of essential amino acids for intracellular growth and free heme as a by-product. In its labile form, free heme is toxic due to its ability to induce free radical formation. Parasites counter this toxicity by converting heme into inert hemozoin (Hz) crystals [12]. Extensive evidence shows that 4-AQ drugs such as chloroquine (CQ) and piperaquine (PPQ) exert their antiplasmodial activity by accumulating within the DV and binding to heme monomers and dimers, effectively interfering with this detoxification pathway [13]. This antiplasmodial activity is predicated on the structurally unique pharmacophore of these compounds that comprises the 4-amino-7-chloroquinoline nucleus for heme binding and inhibition of Hz formation as well as a tertiary amino group in the side chain for vacuolar drug accumulation [14,15]. However, point mutations in the *P. falciparum* chloroquine resistance transporter (PfCRT) [16], an oligopeptide and drug transporter located on the DV membrane [17], have been identified as the main driver of resistance to CQ, PPQ, and some related quinolines [18]. Polymorphic PfCRT variants carry 4 to 10 mutations that can differentially modify parasite susceptibility to CQ and PPQ [19,20]. However, several 4-AQs maintain similar activity against both CQ-sensitive and CQ-resistant parasites, suggesting that they are not recognized and exported by mutant PfCRT [21]. This has informed the introduction of more versatile and potent 4-AQs like amodiaquine, pyronaridine, and ferroquine in clinical use as effective alternatives to address resistance [22].

Herein, we identify the multistage antiplasmodial activity of LDT-623. This compound is a side-chain-modified 4-AQ structurally analogous to LDT-611 that was previously identified in a screening campaign on a library of ~120,000 natural products and derivatives for potential antiplasmodial activity [23]. To evaluate the activity of LDT-623 against other stages of the *P. falciparum* lifecycle, we tested its gametocytocidal potential and ability to inhibit other exo-erythrocytic forms of the parasite. Furthermore, we investigated its MoA and possible cross-resistance with known drug targets. Our results open up the possibility of further exploring this compound as a potential antimalarial.

2. Material and methods

2.1. Compound preparation

Screening compounds were purchased from providers Chembridge, MedChemExpress, Inter-BioScreen, ChemDiv Inc, and BLD Pharmatech Ltd, through the MolPort website (www.molport.com) and were further dissolved in DMSO in 10 mM stock solutions. Standard antimalarial drugs were purchased from Sigma-Aldrich and prepared as 10 mM stocks.

2.2. Virtual screening workflow for the identification of LDT-611 structural analog molecules

Based on the premise that structurally similar compounds may possess similar biological activity, we carried out a virtual screening of the MolPort library of ~7.5 million compounds to select molecules with relevant structural similarity to LDT-611. We employed the "Find similar" function that utilizes the Tanimoto coefficient, a quantitative measure of chemical scaffold

similarity, to filter molecules with structural similarity. A similarity cutoff of 78% ($T_c = 0.78$) was defined based on a visual inspection of analog compounds, to keep those that were 4-AQ and resembled LDT-611's structure. Further steps removed double entries and molecules whose antimalarial activity had been previously reported on PubChem. A final filter removed acridines from the dataset. Finally, the selected analogs were purchased and evaluated *in vitro*.

2.3. *P. falciparum in vitro* culture and ABS assays

P. falciparum ABS parasites were cultured at 3% hematocrit in human O^+ RBCs in RPMI-1640 media supplemented with 25 mM HEPES, 50 mg/L hypoxanthine, 2 mM L-glutamine, 0.21% sodium bicarbonate, 0.5% (w/v) AlbuMAXII (Invitrogen) and 10 µg/mL gentamycin. Culture flasks were kept in modular incubator chambers (Billups-Rothenberg) in a 5% O_2, 5% CO_2, and 90% N_2 atmosphere at 37˚C. Synchronized ring-stage parasites were obtained by two consecutive rounds of treatment with 5% D-sorbitol in 48-hour intervals [24]. ABS parasite survival assays were performed to define half-maximal compound concentrations that inhibit 50% or 90% parasite growth (IC_{50} and IC_{90}). This was done by exposing cultures at 1% hematocrit and 0.3% parasitemia in 96-well plates in the presence of drugs in a two-fold 10 or 12-point serial dilution in duplicate along with drug-free controls. After a 72-hour incubation, parasite survival was assessed by flow cytometry on an iQue flow cytometer (Sartorius) using SYBR Green and MitoTracker Deep Red FM (Life Technologies) as nuclear stain and vital dye, respectively. Parasite survival was determined as a percentage relative to drug-free control. IC_{50} values were interpolated from log concentration *versus* response curves in Prism 9 (GraphPad Prism Software Inc.).

2.4. Cytotoxicity assays

Human hepatoma (HepG2) and fibroblast-like monkey kidney cells (COS-7) were cultured in Dulbecco's Modified Eagle Medium supplemented with 10% heat-inactivated fetal bovine serum and gentamycin (40 mg/L) at 37˚C in a 5% CO_2 atmosphere. Cytotoxicity of test compounds was measured by metabolic reduction of mitochondrial enzymes using the MTT assay (3-[4,5-dimethyl-thiazol-2-yl]-2,5-diphenyltetrazolium chloride) [25]. Cells were seeded at 10^5 cells/well in 96-well plates and incubated for 72 hours in the presence of a 2-fold 12-point serial dilution of drugs along with drug-free controls. After adding 15 µL of MTT (5 mg/mL) to the wells, plates were centrifuged at 317g for 5 minutes and the pellet was resuspended in isopropanol. Absorbance was measured at 570 nm (CLARIOStar, Labtech BMG). Cell viability was determined by formazan production, and was expressed as a percentage of untreated control wells.

2.5. *P. falciparum* gametocyte production and growth inhibition assay

P. falciparum NF54-Pfs16-GFP-Luc (MRA-1217), a highly gametocyte-producing strain, was cultured following standard procedures [26]. NF54-Luc ABS parasites were sorbitol-synchronized as previously described [24] and cultured to reach 8–10% parasitemia as mature trophozoites prior to starting gametogenesis induction via nutrient deficit stress [27]. Briefly, stress was induced by replacing only 40% of the culture medium and returning cultures to a 37˚C incubation. Cultures were treated with 50 mM N-acetylglucosamine for 10 days to remove ABS parasites. Mature gametocytes (stages IV-V) were isolated using magnetic columns and incubated at 2% gametocytemia and 1.5% hematocrit in 96-well plates containing the test compounds for 48 hours at 37˚C, following standard *P. falciparum* culturing conditions. Methylene blue was used as a gametocytocidal control alongside drug-free wells. Luciferase activity was assessed by adding 40 µL of luciferin substrate (Promega) to 40 µL of parasite lysates and

detecting bioluminescence at an integration constant of 10s with the BioTek Cytation 5 Cell Imaging Multimode Reader [28].

2.6. *In vitro* inhibition of *P. berghei* ookinete formation

To measure the inhibition of gamete conversion into ookinetes, a mutant luciferase-expressing *P. berghei* line (nLuc) was intraperitoneally injected into BALB/c mice [29]. After 3–4 days, gametocyte-carrying blood samples were collected. *In vitro* compound testing was carried out by exposing 4 μL of infected blood mixed with 80 μL of culture medium (RPMI-1640 supplemented with 25 mM HEPES, 50 mg/L hypoxanthine, and 1% penicillin/streptomycin/neomycin at pH 8.3) to a range of drug concentrations for 24 hours at 21°C. Following the incubation, 20 μL of nLuc substrate (Nano-Glo Luciferase Assay System, Promega) was added to each well, and luminescence was measured in a luminometer. Increased light emission correlated with nLuc production and subsequent luciferase activity due to *in vitro* fertilization and ookinete conversion, as luciferase expression in this parasite line is regulated by the CTRP promoter that is ookinete-specific [30]. Conversion inhibition was calculated as the percentage of luciferase activity of drug-exposed wells relative to untreated ones, from which IC_{50} values were interpolated.

2.7. *In vitro* inhibition of liver stage infection

In vitro inhibition of *Plasmodium* liver stage infection was assessed using bioluminescence data from Huh-7 cells infected with a firefly-luciferase-expressing *P. berghei* line, *Pb*GFP-Luc-con [31], in the presence of various compound concentrations. Huh-7 cells, a human hepatoma cell line, were cultured in RPMI-1640 medium supplemented with 10% fetal bovine serum, 1% nonessential amino acids, 1% glutamine, 1% penicillin/streptomycin and 10 mM HEPES at pH 7 at 37°C under 5% CO_2. One day before drug treatment and infection, 10^4 Huh-7 cells/well were seeded in 96-well plates. The medium was then replaced by an infection medium (culture medium supplemented with 50 μg/mL gentamycin and 0.8 μg/mL amphotericin B) containing desired concentrations of test compounds. Fresh sporozoites recovered from salivary glands of infected female *Anopheles stephensi* mosquitoes were added to seeded Huh-7 cells at a 1:1 proportion, followed by centrifugation at 1700g for 5 minutes and incubation for 46 hours at 37°C under 5% CO_2. Compound toxicity against Huh-7 cells was assessed by measuring cell confluency using the Alamar Blue assay (Invitrogen). IC_{50} values were calculated using nonlinear regression analysis (GraphPad Prism version 9).

2.8. PfCRT transport measurement assays

Purified PfCRT variants were reconstituted in preformed liposomes made of *E. coli* total lipids: cholesteryl hemisuccinate 97:3 (w/w) at a protein-to-lipid ratio of 1:150 (w/w). The lumen of the proteoliposomes was composed of 100 mM KPi, pH 7.5, and 2 mM β-mercaptoethanol. Uptake of $[^3H]$CQ (1 Ci/mmol) or $[^3H]$PPQ (1 Ci/mmol) was performed by diluting PfCRT-containing proteoliposomes (30 ng of PfCRTper reaction) in an uptake buffer containing 100 mM Tris/MES, pH 5.5, in the presence or absence of 1 μM of the test compounds. In addition, 1 μM valinomycin was added to the reaction to generate a K^+ diffusion potential-driven membrane potential ($\Delta\Psi$). Reactions were stopped after 30 seconds by the addition of ice-cold 100 mM KPi, pH 6.0, and 100 mM LiCl, and filtered through 0.45-μm nitrocellulose filters (Millipore). Filters were dried and incubated in a scintillation cocktail, and the radioactivity captured on the filters was counted in a Hidex SL300 scintillation counter. The efficiency of detection was calculated with a standard curve of known concentrations of each radiolabeled compound, and this was used to transform decays per minute (dpm) into pmol. The

nonspecific interaction of each compound with nitrocellulose filters was determined by measuring mock uptake in the absence of liposomes or proteoliposomes. These values (determined for each experiment) were used to calculate background uptake in liposomes or proteoliposomes. Drug-specific uptake was determined by subtracting the time-dependent accumulation of the tested compounds in control liposomes (lacking PfCRT) from that measured in PfCRT-containing proteoliposomes [20].

Solid Supported Membrane (SSM)-based electrophysiological measurements were performed using SURFE^{2}R N1 technology (Nanion Technologies, Inc.) according to published protocols [32,33]. Briefly, sensors were coated with 1-octadecanethiol (Sigma-Aldrich), rinsed, and 1,2-diphytanoyl-sn-glycero-3-phosphocholine (Avanti Polar Lipids, Inc) was added. Immediately, the sensor was filled with 50 μL non-activating buffer (10 mM Tris-MES, pH 5.5) and PfCRT-containing proteoliposomes (PLs). To generate a K^+ diffusion potential-driven $\Delta\Psi$, valinomycin was included at a final concentration of 80 nM [34,35]. The activating solution (10 mM Tris-MES, pH 5.5 containing either 10 μM CQ, PPQ, LDT-623, pyrimethamine, or atovaquone) was applied using a single-solution exchange protocol (activating buffer incubation for 1 second). Each measurement was repeated at least twice employing at least three different sensors. Peak currents for PfCRT were corrected by subtracting the peak currents recorded with control liposomes (lacking this transporter). To acquire the PfCRT-elicited charge (Coulomb) movement associated with drug transport, the area under the curve (current as a function of time) was analyzed with GraphPad Prism version 10.

2.9. Cellular heme fractionation assay

A heme fractionation assay was used to measure the inhibition of Hz formation in cultured ABS *P. falciparum* 3D7 parasites as previously described [36]. Briefly, ring-stage 3D7 parasites were treated with consecutive D-sorbitol and Percoll solutions to obtain tightly synchronized 3 hours post-invasion young rings that were incubated with test drugs (0.5–$3.0 \times IC_{50}$) alongside a vehicle control in standard culturing conditions (see above). Late trophozoites were harvested after 32 hours of incubation by lysing RBCs with 0.05% saponin followed by multiple washes with $1 \times$ PBS (pH 7.5) to remove any residual traces of hemoglobin. The parasite pellet was resuspended in PBS and the total number of trophozoites isolated was quantified using flow cytometry. Contents of the trophozoite pellet were released by hypotonic lysis and sonication. After centrifugation, treatments with HEPES buffer (pH 7.4), sodium dodecyl sulfate, pyridine, and NaOH, allowed us to separate the fractions corresponding to the different heme species of interest. A microplate reader was employed to measure the UV-visible spectrum of each heme fraction as a Fe(III)heme-pyridine complex. Fractions of undigested hemoglobin, "free" heme, and Hz were quantified using a heme standard curve based on the mass of each heme-Fe species per mature trophozoite (fg/cell), obtained by dividing the total amount of each heme species by the corresponding number of parasites in that fraction as determined by flow cytometry. Statistical comparisons and analyses for trends employed Students' *t*-tests (GraphPad Prism version 9).

2.10. Resistance selection experiments

Resistance to LDT-623 was assessed using single-step *in vitro* resistance selection protocols [37]. Duplicate flasks with 1×10^9 *P. falciparum* Dd2-Pol δ parasites were exposed to $3 \times IC_{50}$ under two different drug regimens: (1) removal of drug pressure as soon as live parasites cleared, and (2) drug pressure kept constant throughout the experiment. Dd2-Pol δ is a hyper-mutable line with two point mutations in DNA polymerase δ that compromise its proofreading activity [38] Cultures were monitored daily by thin blood smears until live parasites were

no longer detectable. Drug-containing media was changed daily until parasites cleared, and every other day thereafter. Cultures were passaged once weekly by reducing the volume by 25% and replacing 1/3 of RBCs. Recrudescence monitoring was carried out twice a week by thin blood smears for 60 days. In the event of recrudescence, parasite susceptibility to LDT-623 was tested as described above.

2.11. Resistome growth assay

The resistome growth assay employs a parasite pool consisting of 51 barcoded lines including both Dd2 and 3D7 genetic backgrounds, with wild-type lines for both (S3 Table). Most lines used were derived from *in vitro* resistance selection experiments, with others having been CRISPR edited. All lines were barcoded via CRISPR editing of a 101bp barcode cassette into the non-essential *pfpare* locus (PF3D7_0709700) [39]. Parasites were cultured in RPMI-1640 medium supplemented with HEPES (5.94 g/L), $NaHCO_3$ (2.1 g/L), glutamax (1×), hypoxanthine (50 mg/L), gentamycin (25 µg/L), and AlbumaxII (5 g/L) at a 50% hematocrit. Parasite growth was monitored over 14 days by flow cytometry (Cytoflex, Beckman Coulter) by staining with 1× SYBR Green and 0.2 µM MitoTracker Deep Red. Parasitemia adjustments were made to maintain a healthy range of <5% parasitemia. Parasite cultures were harvested at day 14 and lysed by saponin (0.05%), with pellets washed twice with PBS. Barcodes were PCR amplified using 5 µL of parasite pellet and sequenced by Illumina amplicon sequencing [40].
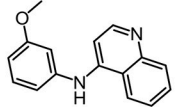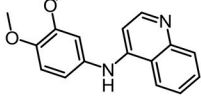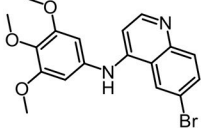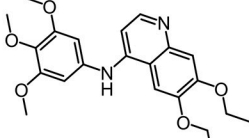
3. Results
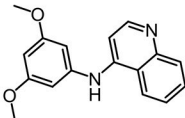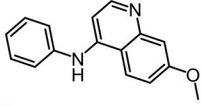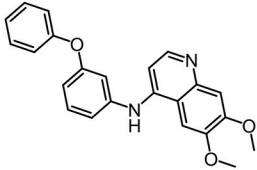
3.1. Identification and activity profiling of LDT-611 and its analogs

In a previous study, we identified several biodiversity-derived compounds with *in vitro* activity against *P. falciparum* ABS parasites *in vitro* [23]. To further explore the antimalarial potential of these hits, we chose LDT-611 (S1A Fig) due to the combination of its sub-micromolar activity against ABS parasites, selectivity index > 10, and relatively low structural similarity to clinical antimalarials. LDT-611 inhibited the growth of CQ-sensitive (3D7) and CQ- and mefloquine-resistant (W2) parasite strains with IC_{50} values of 760 and 820 nM, respectively (S1B Fig). Its equipotency against wild-type and mutant PfCRT isoforms suggests that this compound can circumvent CQ resistance. To identify a more potent compound, we used the Tanimoto coefficient as part of an optimization pipeline that yielded 11 available analogs (S1C Fig). Tanimoto coefficients (S1D Fig) showed that at least 78% of their structures were shared ($T_c = 0.78$), with the potent antimalarial 4-AQ nucleus remaining intact. These 11 analogs were then evaluated for their activity against *P. falciparum* 3D7 and Dd2 ABS parasites, along with cytotoxicity assays with COS-7 and HepG2 mammalian cell lines (Fig 1).

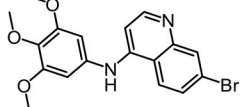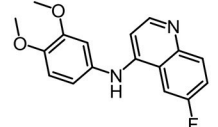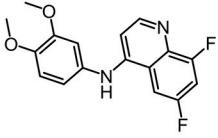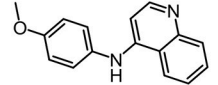### 3.2. LDT-623, the most potent analog, exhibits multistage antiplasmodial activity

LDT-623 was the most potent of the analogs tested against ABS parasites, with IC_{50} values of 127 and 365 nM for 3D7 and Dd2 ABS parasites, respectively) (Fig 2A). This compound was therefore selected for further experimental evaluation throughout the *Plasmodium* lifecycle (S1 Table).

The potential transmission-blocking activity of LDT-623 was assessed by exposing NF54 stage IV-V gametocytes to 5 µM of test compounds. LDT-623 inhibited 62% of mature gametocyte viability compared to untreated control (Fig 2B), an unusual activity for 4-AQs [41]. Gametocytocidal activity was assessed alongside methylene blue, a positive control that showed 100% activity at the same 5 µM concentration. We also employed a *P. berghei* model to

Code	2D structure	IC$_{50}$ [a] (µM)		CC$_{50}$ [b] (µM)	
		3D7	Dd2	COS-7 (SI [c])	HepG2 (SI [d])
LDT-617		1.8 ± 0.1	1.9 ± 0.2	51.2 ± 6.6 (28.9)	40.8 ± 12.2 (23.1)
LDT-618		1.8 ± 0.1	1.9 ± 0.2	> 100 (> 56.5)	29.8 ± 9.7 (16.8)
LDT-619		> 5	> 5	3.3 ± 0.3 (0.7)	0.3 ± 0.04 (0.1)
LDT-620		0.4 ± 0.05	0.5 ± 0.1	2.6 ± 0.3 (6.3)	1.6 ± 0.1 (3.8)
LDT-621		2.2 ± 0.1	2.0 ± 0.3	6.5 ± 4.2 (2.8)	0.5 ± 0.1 (0.2)
LDT-622		0.2 ± 0.02	0.4 ± 0.06	3.8 ± 0.7 (17.5)	3.0 ± 0.9 (13.7)
LDT-623		0.13 ± 0.01	0.3 ± 0.03	0.5 ± 0.1 (3.8)	1.3 ± 0.1 (10)
LDT-624		1.6 ± 0.7	1.0 ± 0.2	41.3 ± 17.2 (26.1)	32.5 ± 7.5 (20.6)
LDT-625		3.2 ± 0.8	2.9 ± 0.5	20.4 ± 1.3 (6.2)	33.3 ± 3.8 (10.3)
LDT-626		5.5 ± 0.5	3.2 ± 0.4	50.9 ± 22.2 (9.3)	53.8 ± 10.8 (9.8)
LDT-627		2.5 ± 0.8	2.0 ± 0.2	54.5 ± 16.7 (22.1)	12.7 ± 6.4 (5.2)

Fig 1. *In vitro* activity of LDT-611 analogs against *P. falciparum* asexual blood stages and mammalian cell lines. [a] IC$_{50}$: Mean half-maximal inhibitory concentration and their respective standard errors, assayed against *P. falciparum* 3D7 and Dd2 ABS parasites (N = 3); [b] CC$_{50}$: Mean half-maximal cytotoxic concentration against mammalian cell lines (N = 3); [c] SI: Selectivity index was calculated by dividing the CC$_{50}$ (against COS-7) by the IC$_{50}$ (against 3D7); [d] SI: Selectivity index was calculated by dividing the CC$_{50}$ (against HepG2) by the IC$_{50}$ (against 3D7). Data are represented by mean ± standard deviation.
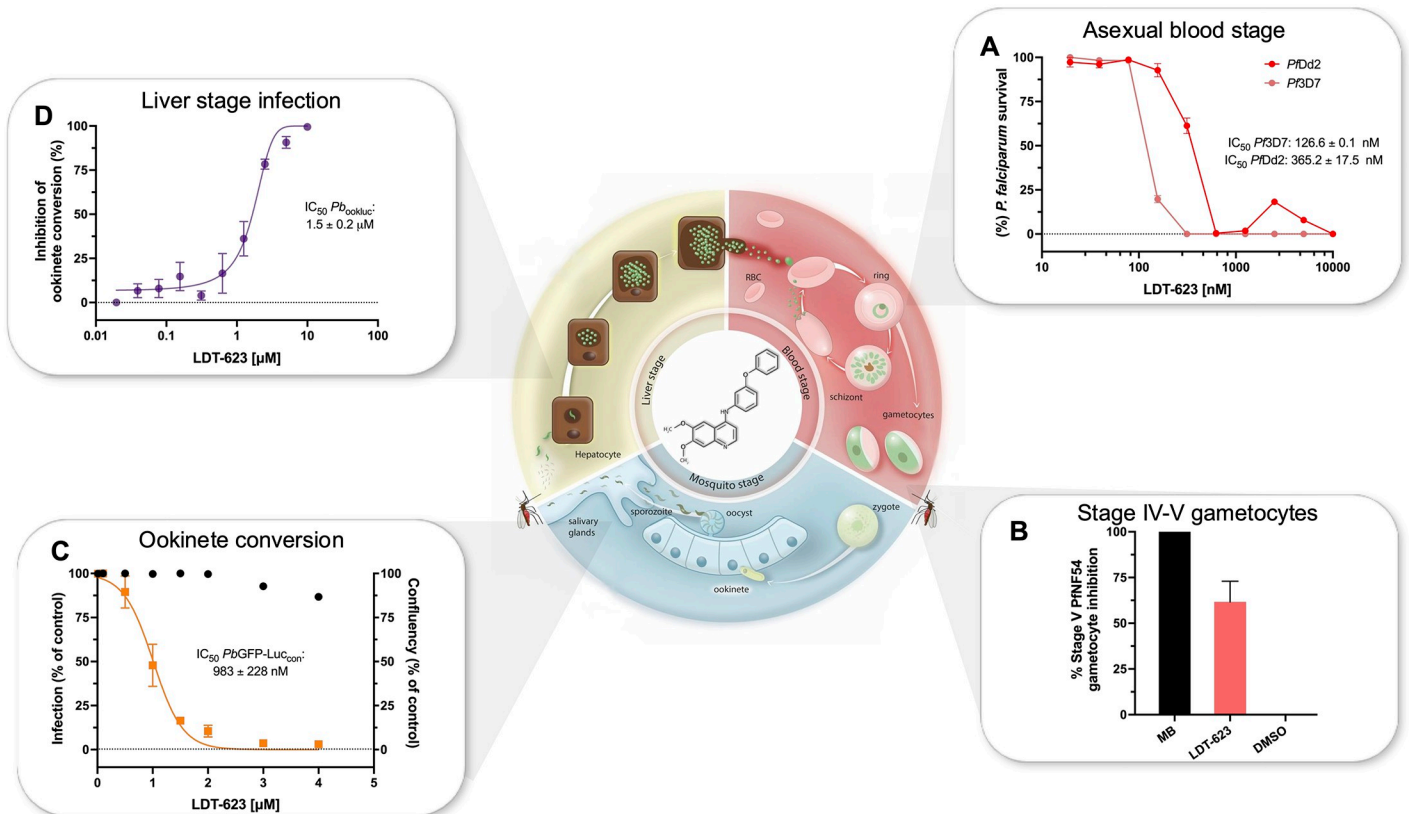
Fig 2. Antiplasmodial activity of LDT-623 throughout the *Plasmodium* lifecycle. (A) LDT-623 *in vitro* activity against ABS *P. falciparum* CQ-sensitive 3D7 and CQ-resistant Dd2 strains. Mean IC$_{50}$: 126.6 and 365.2 nM, respectively. Parasite survival was calculated as a percentage of untreated control. Data represent mean ± SEM (N = 2–3 independent assays, with technical duplicates). (B) Percent activity of LDT-623 against late-stage *P. falciparum* NF54 gametocytes at 5 μM. Gametocyte viability was assessed via bioluminescence. Data represent mean ± SEM (N = 3). MB: methylene blue; DMSO: dimethyl sulfoxide. (C) Dose-response curve for LDT-623 concentration *versus* inhibition of *P. berghei* ookinete formation compared to vehicle-treated control. IC$_{50}$: 1.5 μM. Data represent mean ± SEM (N = 7). (D) Pre-erythrocytic activity of LDT-623. IC$_{50}$: 983 nM. Dose-response curve represents hepatic stage infection as a percentage of drug-free control assessed by luminescence 48h after infection of Huh-7 cells with *P. berghei* sporozoites, while black dots express host cell confluency. Data represent mean ± SEM (N = 2).

evaluate LDT-623's inhibition of ookinete formation *in vitro*, using a conversion assay that evaluates the inhibition of gamete fertilization into a zygote and subsequent conversion into an ookinete. LDT-623 yielded an IC$_{50}$ of 1.5 μM (Fig 2C). For reference, CQ inhibited 56.7% of zygote conversion into ookinetes at 10 μM (S2 Fig).

We also observed pre-erythrocytic activity of LDT-623 using an *in vitro* firefly luciferase-expressing *P. berghei* line by measuring inhibition of hepatocyte infection based on luminescence intensity [31]. In agreement with its IC$_{50}$ of 983 nM (Fig 2D), LDT-623 showed 52.1% inhibition of hepatic infection at 1 μM. The positive control atovaquone almost completely ablated infection at 10 nM, consistent with its known liver stage activity [42]. Of note, we observed minimal to no dose-dependent toxicity towards Huh-7 host cells, as evidenced by over 86% cell viability at the maximum concentration of 4 μM LDT-623.

3.3. LDT-623 inhibits intracellular hemozoin formation

The 4-AQ nucleus, contained by antimalarial drugs such as CQ and PPQ, interferes with the heme detoxification pathway inside the parasite DV through complexation with heme, leading to inhibition of Hz formation [43,44]

Heme fractionation profiling of LDT-623 revealed a statistically significant increase in "free" heme in a concentration-dependent manner compared to untreated control (Fig 3A and S2 Table). Concurrently, we also observed significant concentration-dependent decreases in the levels of Hz. Moreover, an augmented percentage of undigested Hb was observed starting at $0.5 \times IC_{50}$ of LDT-623. CQ, used as a positive control, also exhibited a significant increase in "free" heme starting at $0.5 \times IC_{50}$ while Hz levels only decreased significantly from $2 \times IC_{50}$. Interestingly, the proportion of "free" heme present as undigested Hb within the DV after incubation was significant at $2.5 \times IC_{50}$ of CQ only (Fig 3B). As a negative control, parasites were treated with KAE609 (cipargamin), a PfATP4 inhibitor, which did not affect Hz formation [45]. Besides a subtle yet significant increment in Hb levels observed under 2 and $2.5 \times IC_{50}$, no striking perturbations were noted for any of the heme species investigated under KAE609 treatment (Fig 3C). Altogether, these results demonstrate that LDT-623 interferes with the vital Hz formation pathway, presumably due to its quinoline core.
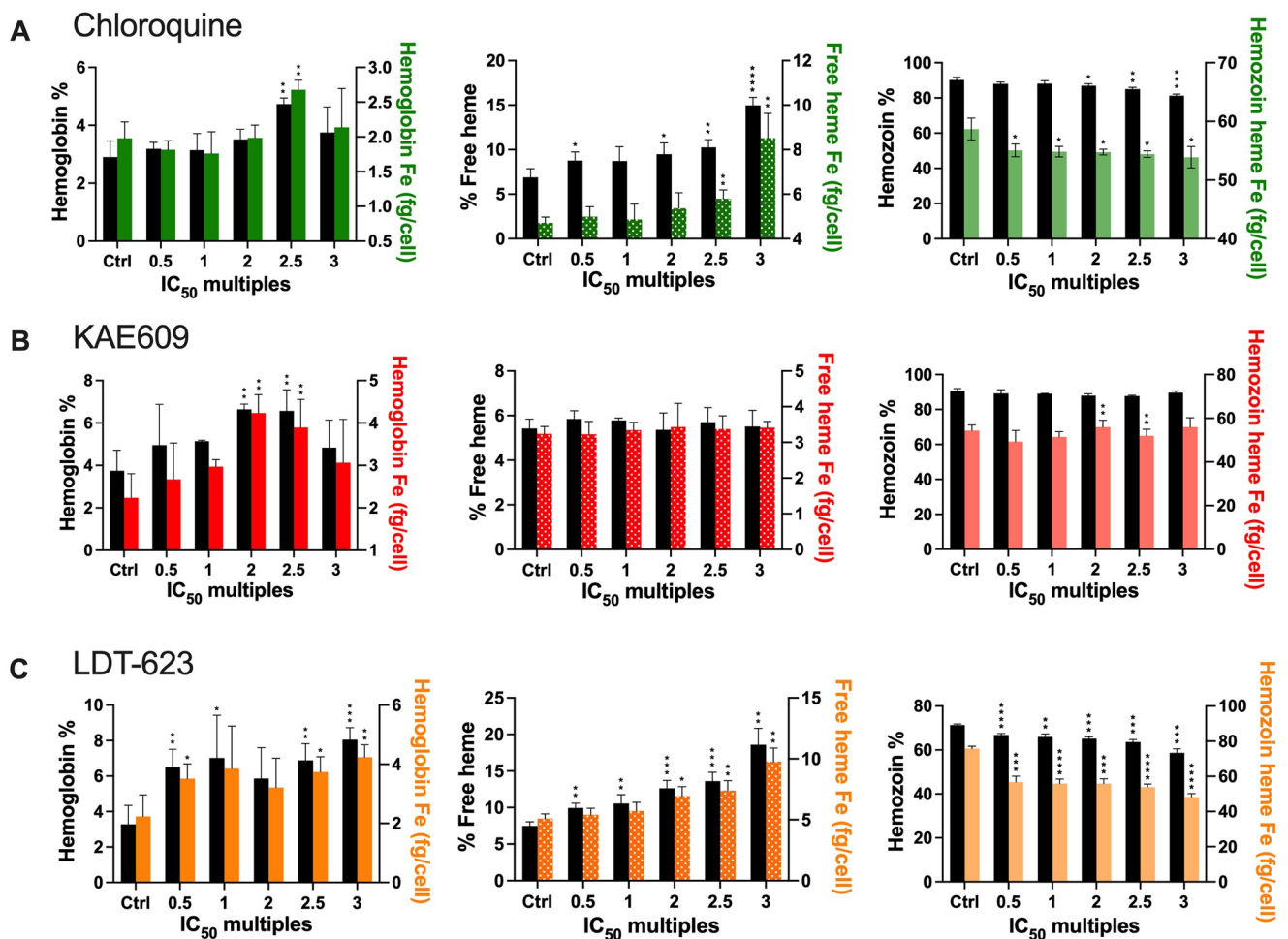
Fig 3. LDT-623 interferes with the hemozoin formation pathway within the digestive vacuole. (A) Parasites treated with LDT-623 display a more pronounced heme fractionation profile than CQ. (B) Heme fractionation profile of CQ-treated *P. falciparum* 3D7 parasites showing an increase in free heme and a decrease in Hz, as determined 32 h post-drug exposure. (C) KAE609 treatment did not interfere with heme or Hz accumulation. Percent levels of heme species (hemoglobin, free heme, or hemozoin) are represented by the black bars on the left y-axis, and absolute heme amounts (hemoglobin Fe, free heme Fe, or hemozoin heme Fe) determined from a heme standard curve and measured in femtograms per cell are represented in different colors (LDT-623 in red, CQ in orange, and KAE609 in green) on the right y-axis. Statistical comparisons of the drug-treated lines with their untreated controls were performed using two-tailed Student's tests (with Welch's correction). *p < 0.05; **p < 0.01; ***p < 0.001; ****p <0.0001.

https://doi.org/10.1371/journal.ppat.1012627.g003

3.4. LDT-623 impacts PfCRT variant-specific drug efflux

PPQ and CQ resistance-conferring mutations in PfCRT allow positively charged drugs and other solutes to efflux into the cytosol [20,46]. Consequently, CQ- or PPQ-resistant parasites accumulate lower amounts of drugs within their DVs and prevent inhibition of heme detoxification. This contrasts with drug-sensitive parasites, where the increased intravacuolar concentrations of these drugs inhibit heme detoxification and result in subsequent parasite death.

Using PfCRT-containing proteoliposomes as a surrogate for drug transport, we employed an assay that mimics an "inside-out" parasite DV. This assay employed the CQ-resistant, PPQ-sensitive 7G8 PfCRT isoform, as well as two variants (7G8^{F145I} and 7G8^{C350R}) that include an additional mutation that is observed in Southeast Asia and South America, respectively, and that mediate PPQ resistance and a reversion to CQ sensitivity [19,47]. Assays were designed to evaluate the impact of LDT-623 on PfCRT-mediated drug uptake in these 7G8 isoforms. The uptake of [^{3}H]CQ or [^{3}H]PPQ was measured in PfCRT-containing proteoliposomes using an internally directed pH gradient and $\Delta\Psi$ (Fig 4A) and was normalized to that of control liposomes lacking PfCRT [20]. Drug-specific transport (here measured by [^{3}H]-labeled drug accumulation) can be differentially mediated by distinct PfCRT isoforms, in agreement with varying resistance phenotypes as seen with the PfCRT isoforms used: 7G8^{7G8} (CQ-resistant, PPQ-sensitive), 7G8^{F145I} (CQ-sensitive, PPQ-resistant) and 7G8^{C350R} (CQ-sensitive, PPQ-resistant).

In the CQ-resistant 7G8 PfCRT isoform, the drug-free control showed that [^{3}H]CQ uptake was maximal, as expected, based on its resistance phenotype (S3 Table). The addition of 1 μM LDT-623, however, reduced the uptake of [^{3}H]CQ (to an average of 60.2% relative to [^{3}H]CQ without another drug) (Fig 4B). As for the PPQ-resistant 7G8^{F145I} and 7G8^{C350R} isoforms, the addition of [^{3}H]CQ also yielded a reduced percentage of [^{3}H]PPQ uptake (30.% and 47.2%, respectively, relative to [^{3}H]PPQ alone) (Fig 4C and 4D). No competitive inhibition of [^{3}H]CQ or [^{3}H]PPQ transport was observed with pyrimethamine (PYR) or atovaquone (ATQ), which have entirely distinct MoAs (inhibition of folate synthesis and the mitochondrial electron transport chain, respectively). Of note, [^{3}H]CQ uptake by the PfCRT 7G8 isoform and [^{3}H]PPQ uptake by the 7G8^{F145I} and 7G8^{C350R} isoforms were inhibited by the addition of the reciprocal agents PPQ and CQ (see Fig 4B–4D), to levels slightly greater than those observed with LDT-623. We interpret these data as evidence that PPQ and CQ can antagonize each other's transport via appropriately mutated PfCRT variant isoforms. Earlier studies have shown that PPQ and CQ can bind drug-resistant and -sensitive PfCRT isoforms with similar K_d values, with the difference being that the resistant isoforms acquire transport properties [20].

Since both [^{3}H]CQ and [^{3}H]PPQ uptake are reduced in the presence of LDT-623 in the PfCRT isoforms tested herein, it can be speculated that LDT-623 competes with CQ and PPQ for transport by the distinct PfCRT isoforms. This notion is supported by the robustness of variant-specific 4-AQ interactions with PfCRT and by the minimal impact of ATQ- or PYR–cytochrome *bc1* or dihydrofolate reductase inhibitors, respectively [48,49], on the uptake of [^{3}H]CQ or [^{3}H]PPQ (Fig 4B–4D). To provide further experimental evidence for the interaction of LDT-623 with PfCRT, we established a robust platform to screen electrogenic events in the same PfCRT-containing proteoliposome-based model system using solid-supported membrane (SSM) electrophysiology [33,50]. This system enables the detection of ion fluxes associated with 4-AQ, e.g., CQ, PPQ, or LDT-623, transport. Our data (Fig 4E–4G) reveal that the addition of the three tested 4-AQs to the distinct PfCRT isoforms–as validated with parallel [^{3}H]CQ and [^{3}H]PPQ uptake studies (Fig 4B–4D)–elicited currents. We conclude that these currents, reflective of the change of the membrane potential in the PfCRT-containing
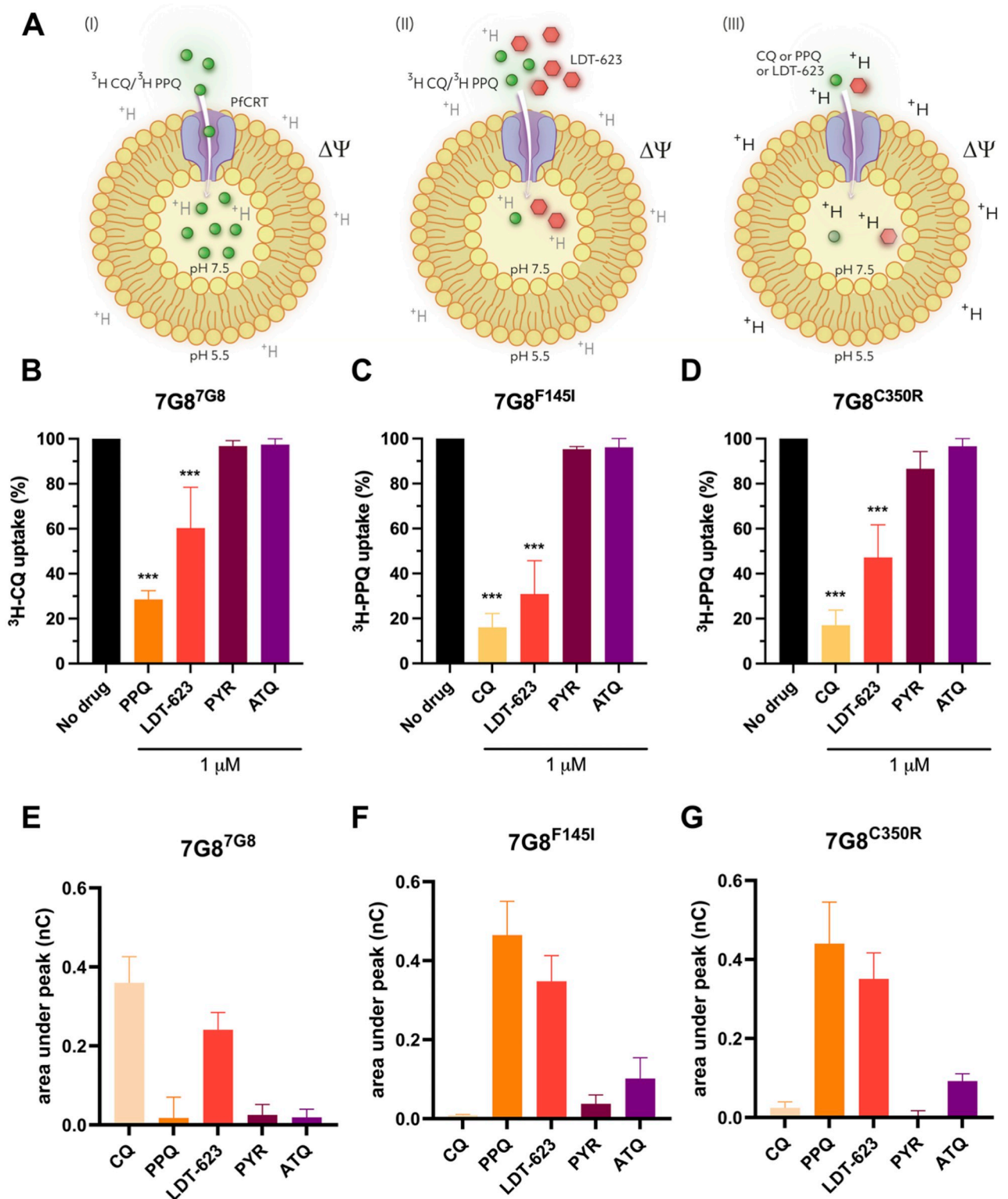
Fig 4. Uptake of the 4-AQs CQ, PPQ, and LDT-623 in PfCRT-containing proteoliposomes. (A) Schematic representation of the drug uptake assay highlighting the "inside-out" digestive vacuole aspect of PfCRT-containing proteoliposomes. Uptake of radiolabeled CQ or PPQ in the absence (I) or presence (II) of LDT-623 using the accumulation of radiolabeled CQ or PPQ as read-out or measuring 4-AQ transport-associated current fluxes (III) with electrophysiology. Uptake of 100 nM [³H]CQ (B) or [³H]PPQ (C-D) measured for 30 seconds in proteoliposomes containing the indicated PfCRT variants normalized to control liposomes. Data represent mean ± SEM of N = 3 independent experiments with n = 7 technical replicates each.

(E-G) Transport of 10 μM CQ, PPQ, LDT-623, PYR, or ATQ by proteoliposomes containing indicated PfCRT variants using the SURFE^{2}R N1-based SSM electrophysiological measurements. Data represent PfCRT isoform-specific currents (corrected for the non-specific signal measured in control liposomes lacking PfCRT) and are the mean ± SEM of N = 3 independent experiments with n = 6–9 technical replicates each.

https://doi.org/10.1371/journal.ppat.1012627.g004

proteoliposomes, are the result of 4-AQ transport-associated flux of protons (H$^+$), according to an H$^+$/4-AQ co-transport (symport) mechanism as we recently demonstrated [20].

3.5. Profiling of LDT-623 in *pfcrt* and *pfmdr1*-edited *P. falciparum* lines illustrate variant-mediated cross-resistance profiles

To correlate drug uptake results with parasite susceptibility phenotypes, we used *pfcrt*-modified isogenic parasite lines previously generated [19,20,51–53] via zinc-finger nuclease editing (Table 1 and Fig 5A). We hypothesized that distinct PfCRT isoforms could display different binding transport activity patterns for 4-AQs, thereby modulating parasite susceptibility to LDT-623.

PfMDR1, another DV-localized transporter, is a major determinant of pleiotropic antimalarial resistance in the field. Studies have shown that changes in both copy number variations and amino acids at position 86 in *pfmdr1* significantly impact parasite susceptibility to several antimalarial drugs [54,55]. Because there appears to be an interplay between specific *pfcrt* and *pfmdr1* alleles [56,57], we also explored the role of genetically manipulated *pfmdr1* on the susceptibility of *P. falciparum* to LDT-623. We used the NF10^{YF} clone (progeny of a genetic cross between 7G8, from Brazil, and GB4 parasites, from Gabon) that harbors a single copy of the GB4 *pfmdr1* allele encoding the N86Y/Y184F (YF) haplotype, and the NF10^{NF} clone, genetically engineered to express the N86/Y184F (NF) haplotype [55]. Additionally, we assessed the impact of *pfmdr1* amplification on the activity of LDT-623 using the parental line FCB and FCB^{KD1} that express two or one copies of *pfmdr1*, respectively [54].

Most of the *pfcrt*-edited *P. falciparum* lines assessed did not show substantial rightward shifts in their survival curves (Fig 5C–5E). For comparison, previously published CQ and PPQ

Table 1. Panel of *pfcrt*-edited *P. falciparum* lines used in this study.

Parasite line	Origin	Phenotype		PfCRT amino acid at listed positions														
		CQ	PPQ	72	74	75	76	93	97	145	218	220	271	326	343	350	353	356	371
Dd2^{Dd2}	SE Asia	R	S	C	I	E	T	T	H	F	I	S	E	S	M	C	G	T	I
Dd2^{T93S}	Cambodia	R	R	C	I	E	T	**S**	H	F	I	S	E	S	M	C	G	T	I
Dd2^{H97Y}	Cambodia	R	R	C	I	E	T	T	**Y**	F	I	S	E	S	M	C	G	T	I
Dd2^{F145I}	Cambodia	S [a]	R	C	I	E	T	T	H	**I**	I	S	E	S	M	C	G	T	I
Dd2^{I218F}	Cambodia	S	R	C	I	E	T	T	H	F	**F**	S	E	S	M	C	G	T	I
Dd2^{M343L}	Cambodia	R	R	C	I	E	T	T	H	F	I	S	E	S	**L**	**C**	G	T	I
Dd2^{G353V}	Cambodia	S	R	C	I	E	T	T	H	F	I	S	E	S	M	C	**V**	T	I
Dd2^{3D7}	Africa	S	S	C	M	N	K	T	H	F	I	A	Q	N	M	C	G	I	R
7G8^{7G8}	S. America, W. Pacific	R	S	S	M	N	T	T	H	F	I	S	Q	D	M	C	G	L	R
7G8^{F145I}	Experimental	S	R	S	M	N	T	T	H	**I**	I	S	Q	D	M	C	G	L	R
7G8^{C350R}	French Guiana	S	R	S	M	N	T	T	H	F	I	S	Q	D	M	**R**	G	L	R

[a] Sensitized to CQ compared to the parental line but not fully sensitive. *pfcrt* editing by customized zinc-finger nucleases was confirmed using Sanger sequencing. Differences from the 3D7 wild-type allele are shown in gray shading for both Dd2 and 7G8. Bold indicates mutations identified from piperaquine-resistant field isolates. S: sensitive, R: resistant. Table adapted from [19,20,51].

https://doi.org/10.1371/journal.ppat.1012627.t001
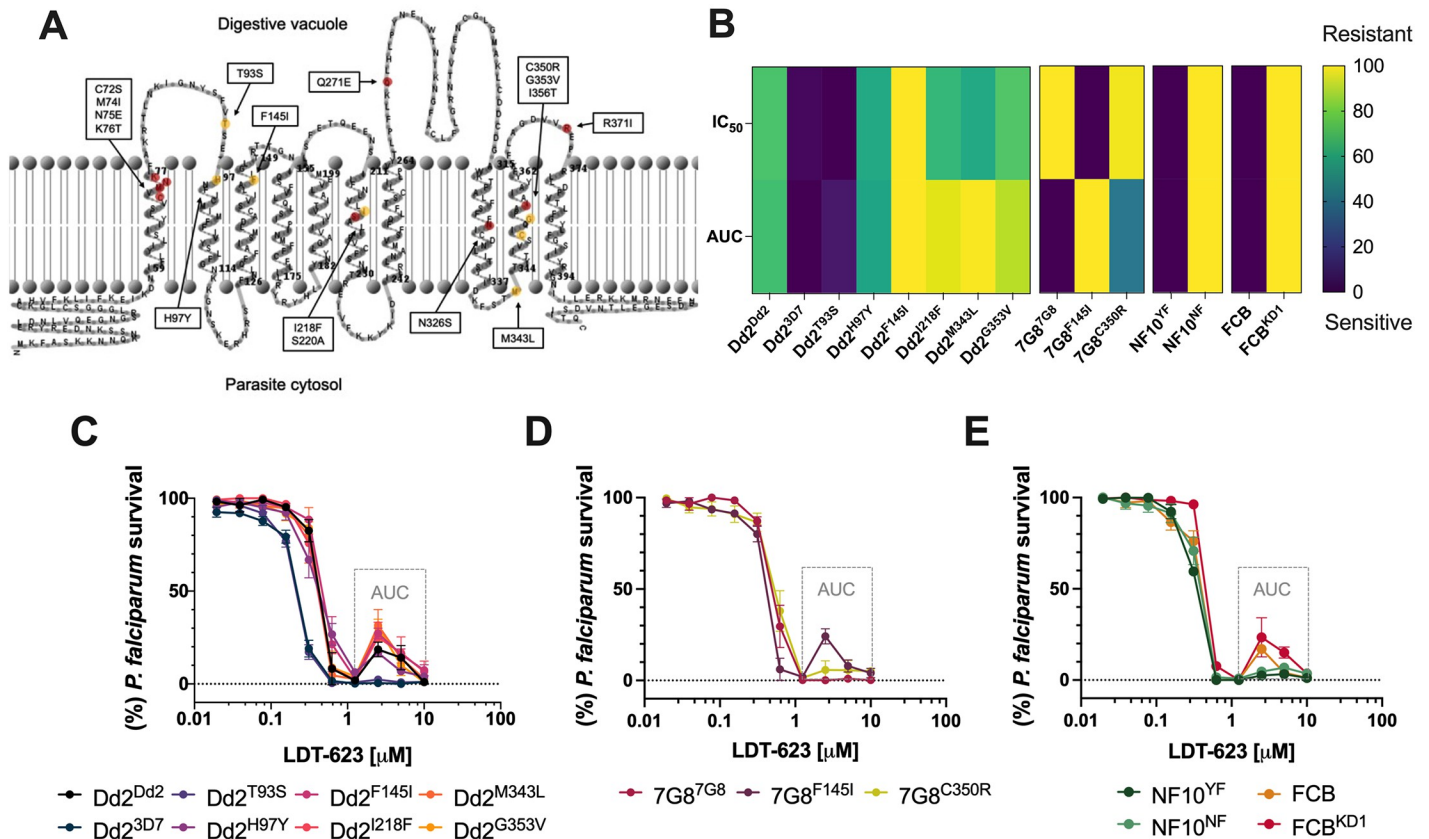
Fig 5. LDT-623 dose–response curves illustrate distinct variant PfCRT-mediated resistance profiles. (A) Mapping of CQ (red) and PPQ (yellow) resistance-conferring PfCRT amino acid substitutions on the 2D structure of PfCRT[3D7] using TMRPres2D [59]. (B) Cross-resistance heatmap of IC_{50} and AUC values for LDT-623 across *pfcrt* and *pfmdr1*-edited *P. falciparum* lines (N = 2–4). Data were normalized across parameters and scaled into a 0–100 interval for heatmap coloring. (C-D) Dose-response curves for *pfcrt*-edited clones. Data show mean ± SEM percent parasite survival (relative to drug-free controls) as a function of LDT-623 concentration (N = 2–4). (D) Dose-response curves for *pfmdr1*-edited clones. Data show mean ± SEM percent parasite survival (relative to drug-free controls) as a function of LDT-623 concentration (N = 3).

susceptibility data for the parasite strains tested were listed alongside LDT-623 results (S4 and S5 Tables). Even though initial LDT-623 concentrations similarly killed different parasite lines, specific sets of mutations differentially impacted parasite survival under higher drug concentrations, resulting in incomplete killing. This incomplete killing phenotype, characterized by biphasic dose-response curves and associated with PPQ resistance [19,58], reveals atypical profiles for typical 72 h dose-response assays, complicating the IC_{90} determination. In this way, AUC was calculated within the region of the survival curve limited by drug concentrations from 1.25 to 10 μM, encompassing a range of biphasic responses. Lower, yet not statistically significant, AUC for Dd2[3D7] and Dd2[T93S] (*p*-value: 0.1, Mann-Whitney U test) suggest an increase in susceptibility to LDT-623 compared to the isogenic Dd2[Dd2] (Fig 5B). 7G8 clones 7G8[F145I] and 7G8[C350R], linked to PPQ resistance, were the closest to statistical significance in the AUC analysis compared to the isogenic 7G8[7G8] (*p*-value: 0.06; Mann-Whitney U test), suggesting a trend towards diminished susceptibility to LDT-623 (Fig 5B). Moreover, the PfCRT F145I mutation seems to play a role in resistance to high concentrations of LDT-623 by protecting parasites via an incomplete killing phenotype, regardless of the parasite's genetic background.

Regarding *pfmdr1* genetic changes, the N-terminal N86 mutation in NF10[NF] did not show any impact on the activity of LDT-623 compared to its parent NF10[YF] at the IC_{50} level (1.1-fold increase, *p*-value: 0.7, Mann-Whitney U-test). While analyzing *pfmdr1* copies, the knockdown clone FCB[KD1] showed a 1.2-fold increase in IC_{50} compared to FCB (Fig 5B), a behavior like that previously observed for CQ [54]. However, this increase was not statistically significant (*p*-value: 0.1, Mann-Whitney U-test). Finally, the knockdown FCB[KD1] displayed a more pronounced biphasic curve compared to its FCB parent but no statistical significance was achieved between their AUC values (*p*-value: 0.4; Mann-Whitney U test). Overall, even though there appears to be a tendency of slight resistance regarding a few of the lines assayed, no striking differences in parasite susceptibility via AUC analysis were observed. None of the *pfcrt* or *pfmdr1* relevant field mutations engineered into these parasite lines yielded significant cross-resistance.

### 3.6. LDT-623 is refractory to resistance selection *in vitro*

In a bid to obtain additional insights into the potential molecular targets or pathways that drive the multistage antiplasmodial activity of LDT-623, we carried out two parallel resistance selection protocols to generate drug-resistant parasites (Fig 6A).

No parasite recrudescence was observed in the set-up where constant pressure was applied throughout the 60 days of selection. In the set-up in which drug pressure was removed after day 7 following parasite clearance, recrudescence was observed in both flasks on day 21. However, drug response assays showed no difference in IC_{50} between the Dd2-Polδ parent culture and the recrudescent bulk parasites from either flask (Fig 6B). Given the biphasic shape of the parasite survival curves, an AUC analysis was performed. While the mean AUC for the Dd2-Polδ parent culture was 35.4, parasites recovered in Flasks 1 and 2 had values of 53.8 and 22.3, respectively (*p*-values: 0.7 and 0.3, Mann-Whitney U test; Fig 6B), revealing no significant difference between the curves (Fig 6C and S6 Table). With no LDT-623-resistant parasites recovered under constant drug pressure, the log minimum inoculum of resistance (MIR) calculated for LDT-623 is higher than 9 (i.e. $>10^9$ infected RBCs), providing evidence for a robust barrier for resistance.

3.7. Failure to recover parasites in the resistome assay indicates no cross-resistance of LDT-623 with major targets and resistance mechanisms

Cross-resistance profiling of compounds against parasite lines with known resistance mutations is another approach to gain insight into the potential resistance liabilities of a compound. Leveraging drug-resistant lines generated predominantly by the MalDA consortium using *in vitro* evolution or genetic engineering has aided the composition of a library of >50 parasites that, altogether, cover a broad range of currently known resistance mechanisms as well as notable targets advancing in the contemporary antimalarial drug discovery pipeline [60–62]. CRISPR-based barcode insertion allowed these representative parasite lines to be pooled and co-cultured, with their relative abundances quantified by barcode sequencing (S7 Table) [40]. Using a multiplexed competitive growth assay, we subjected this pool of barcoded parasites to LDT-623 pressure, as a means to identify potential cross-resistance targets.

Selective pressure of $3 \times IC_{50}$ LDT-623 for Dd2 (~790 nM) was applied to the pool of barcoded parasites and maintained constant throughout the assay. At the same time, cumulative growth profiles were recorded for LDT-623, KDU691 – a known PI4-kinase inhibitor [63], and an untreated control (S3 Fig). After 14 days of incubation, no growth recovery was observed for the pool of barcoded parasites treated with LDT-623 and thus no barcodes could be detected by PCR. In contrast, treatment of the pool with the PI4-kinase inhibitor KDU691 yielded recrudescence after 9 days and enrichment of barcode profiles of PI4-kinase mutant parasites (S3B Fig). Failure of these parasite lines to grow under LDT-623 pressure is a strong
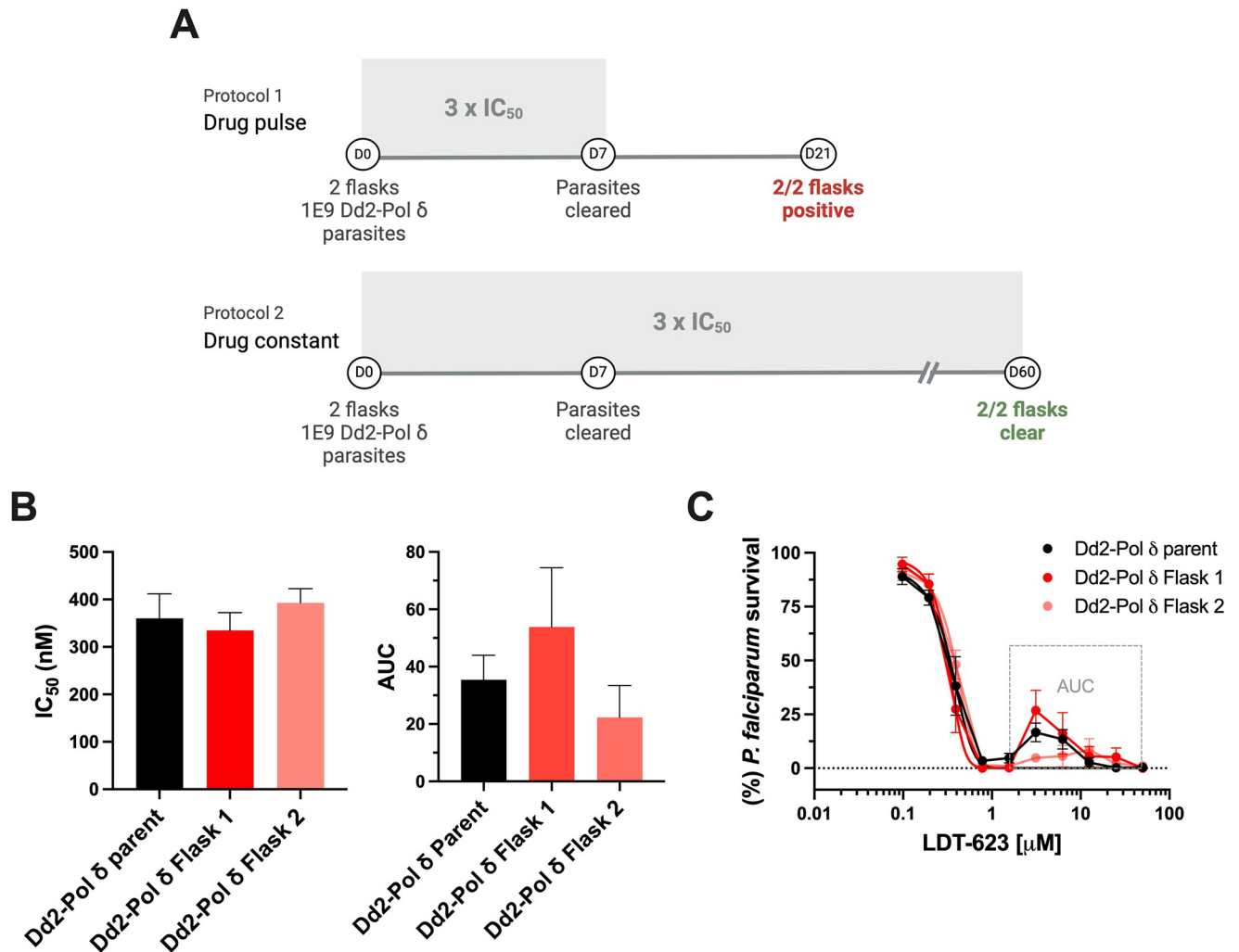
Fig 6. LDT-623 does not readily select for resistance *in vitro*. (A) Selection of resistance to LDT-623 using the Dd2-Polδ line. (A) Parasites were cultured in the presence of 1 μM LDT-623 (~3 × IC$_{50}$). Parasite inoculum was set at 1×10^9 in duplicate flasks. Shading indicated the presence of drug pressure in the protocol. (B) LDT-623 IC$_{50}$ and AUC values for parental and recrudescent Dd2-Polδ lines under LDT-623 pressure. (C) Dose-response curves of LDT-623 for parental line (Dd2-Polδ) *versus* drug-pressured lines (Dd2-Polδ Flask 1 and Dd2-Polδ Flask 2). Arrow represents the $3 \times$ IC$_{50}$ concentration used for resistance selection. Data represent mean ± SEM (N = 5). Statistical significance was determined by Mann-Whitney U tests, *p<0.05.

https://doi.org/10.1371/journal.ppat.1012627.g006

indicator of no cross-resistance with major targets and resistance mechanisms evaluated, such as ABC transporter I (ABCI3), P-type ATPase (ATP4), cyclic amine resistance locus (CARL), and translation elongation factor 2 (eEF2) [64], among others [62] (S7 Table).

4. Discussion and conclusions

Even though 4-AQs have been relatively well-explored, the history of drug development endorses their adoption as partner drugs in antimalarial therapy, as exemplified by amodiaquine, PPQ, and pyronaridine. Based on a previously characterized antiplasmodial molecule [23], a similarity screening coupled with *in vitro* assays identified LDT-623, a 4-AQ with nanomolar ABS activity. Previously described as an ABS inhibitor in high throughput screening endeavors [65], we aimed to explore this molecule's potential by demonstrating its hepatic schizonticidal and transmission-blocking activity in *P. falciparum* mature gametocytes and *P.*

berghei ookinetes. This moderate yet unusual multistage activity that distinguishes LDT-623 from the typical 4-AQ phenotype encouraged us to investigate it further.

Using a cellular heme fractionation assay, we demonstrated that LDT-623 interferes with the heme detoxification pathway within the DV in a concentration-dependent manner. This can be linked to its MoA. Numerous point mutations in *pfcrt* have been proven to mediate CQ [18] and PPQ resistance [66] to varying extents. These mutation-driven phenotypes support parasite evasion from the inhibition of Hz formation within the DV: outward drug transport is significantly greater in PfCRT-mutated forms, leading to a lesser extent of drug accumulation in its site of action, thus rendering the parasite resistant. To further dissect the contribution of these complimentary mechanisms to the MoA of LDT-623, we resorted to isoforms of PfCRT-reconstituted proteoliposomes [20]. Measurement of the active uptake of radiolabeled CQ and PPQ showed that LDT-623 partially interferes with drug transport by PfCRT, suggesting that LDT-623 can compete with the other 4-AQs for their interaction with the same functional site. Indeed, electrophysiological measurements support this notion, as LDT-623 elicits the same magnitude of currents as CQ and PPQ. These currents are considered to reflect PfCRT-mediated H^+-coupled 4-AQ symport, according to which the transport of 4-AQ compounds is associated with the flux of H^+ in the same direction [20].

Functionally, differential drug transport affinities between these PfCRT variants might mirror distinct drug sensitivity profiles. To this end, we put together a panel of *pfcrt*-edited *P. falciparum* lines. To evaluate the potential cross-resistance of LDT-623 with globally relevant *pfcrt* mutations, we selected not only those haplotypes mutated at positions 72–76 from Southeast Asia/Asia (CVIET) and South America (SVMNT) that drive CQ resistance [52] but also PPQ-resistance-conferring mutations such as H97Y, F145I, M343L, or G353V, observed in Southeast Asia [19], and the C350R mutation that has been recently shown to impact over 2/3 of parasite populations analyzed in the Guianas [67–69]. Most Dd2 lines assayed, except for Dd2^3D7 (*wild-type* PfCRT) and Dd2^T93S, show a biphasic response at high LDT-623 concentrations. This same phenotype is not observed in the 7G8^7G8 line with the South American SVMNT PfCRT isoform. We believe that CVIET PfCRT could be the major driver of these bimodal dose-response curves. Overall, we hypothesize that a gain of compound transport by mutant *pfcrt* might be the underlying reason that LDT-623 loses some activity in a range of higher concentrations, as also seen by increased PPQ transport with the highly PPQ-resistant Dd2^F145 and Dd2^T93S parasite lines [20,52]. Although LDT-623 activity hints towards diminished potency against F145I, data is not a proxy for potential clinical settings, as this mutation is highly unfit in the Dd2 background [19] and no reports have shown its emergence in 7G8 parasites.

Because there appears to be an interplay between particular *pfcrt* and *pfmdr1* alleles [56,57], we explored the impact of *pfmdr1*—a marker of resistance to lumefantrine and mefloquine (partner drugs in ACTs), on activity of LDT-623. The FCB line, besides its CVIET PfCRT haplotype, also harbors the *pfmdr1* N86Y mutation (cognate to NF10^YF, yet in a distinct genetic background). Interestingly, although NF10 are also CVIET-bearing parasites, they seem to preserve the sigmoidal curve shape—as opposed to the biphasic response from FCB parasites. Revisiting the trend observed for Dd2 regarding the bimodal curve believed to be driven by CVIET, in this case, we believe that the incomplete killing for both FCB and FCB^KD1 might be due to either a strain-specific behavior or even to possible specific interactions between these *pfcrt* and *pfmdr1* alleles. A few of the mutant PfCRT and PfMDR1 haplotypes evaluated in this study also play a role in the parasite susceptibility to other antimalarial drugs, as seen with increased lumefantrine susceptibility and sensitivity to ART derivatives [70–72]. Additionally, increased *pfmdr1* copy numbers are commonly observed in Southeast Asia [54,72]. These amplified *pfmdr1* copies, fortunately, do not usually extend to African parasite populations,

where the fitness costs potentially do not support their expansion in highly endemic areas [73]. Given that we found no pre-existing cross-resistance with *pfcrt-* or *pfmdr1-*mutated parasites, the results brought by the present study are timely within the context of considering 4-AQs as effective partner drugs. Our finding that inhibition of Hz formation is part of the MoA of LDT-623, along with the absence of the heme detoxification pathway in both liver and insect parasite stages [13] implies a multifaceted MoA, whose basis requires further investigation. Exploring mechanisms of antimalarial compounds beyond ABS is notoriously difficult given the lower parasite loads available in parasite hepatic and sexual stages compared to ABS. Similarly, insect stages are of extremely low density in the mosquito midgut.

We then resorted to hypermutable Dd2-Pol δ ABS parasites that can display an increased mutation rate of up to 28-fold under drug pressure [38], hence expanding the genetic diversity available for the parasite populations during the selective pressure and increasing our chances of identifying a potential separate MoA of LDT-623. Even though this parasite line does not represent a direct proxy for field outcomes, it is a reliable tool to gain further insights into a drug's MoA. This strategy has been successful in generating mutants for antimalarial compounds dubbed "irresistible" [38,74], including ones that have previously failed to select for mutations in 3D7 and Dd2 parasites. The failure of LDT-623 to select resistant parasites *in vitro* suggests that this event might be unlikely to occur in the field. Among numerous potential reasons for this compound not to select for resistance, the bimodal phenotype for LDT-623 recrudescent parasites may reveal a subset of parasites surviving high drug concentrations. This biphasic response could be linked to concentration-dependent activation of drug efflux mechanisms [16,75,76] or even a polypharmacological trait translating into multiple MoAs of this compound [75], which corroborates the multistage antiplasmodial activity observed for LDT-623. Moreover, considering the absence of evidence of lumefantrine and pyronaridine resistance in *P. falciparum* strains to date and the fact that amodiaquine remains widely effective [77], the study is timely when contemplating 4-AQs as effective partner drugs. With ferroquine undergoing phase 2 trials as a first-line partner drug [72,78–82], including in combination with OZ439, revisiting 4-AQs is appealing. In light of this, a novel 4-AQ antimalarial, such as LDT-623, showing no cross-resistance to these relevant genetic changes, may constitute a valuable tool for further drug optimization efforts.

Finally, we explored parasite modulators of LDT-623 susceptibility and gain insight into its MoA using a fitness competition assay employed to identify cross-resistant barcoded parasite lines able to outgrow drug pressure [40]. Strikingly, none of the parasite strains assayed were retrieved. It is also important to mention that compounds like LDT-623, which not only seem to possess a multifaceted MoA but also leverage host-specific processes (such as the heme detoxification pathway) are compelling tools that have the potential to make it more challenging for resistance to evolve [83,84]. Altogether, by leveraging LDT-623's ability to bypass drug efflux mechanisms in mutant PfCRT and PfMDR1, two major resistance determinants in ACT partner drugs, our data encourage revisiting quinolines as components of malaria treatment strategies such as triple ACTs, as demonstrated for other antimalarial combinations [19,51].

Supporting information

S1 Fig. **(A)** Structure of compound LDT-611. **(B)** *In vitro* growth inhibition of chloroquine-sensitive and resistant *P. falciparum* strains for LDT-611 and chloroquine, an antimalarial standard (data are represented as mean ± SD, N = 3). **(C)** Virtual screening workflow for the identification of LDT-611 structural analog molecules. **(D)** Radial plot showing structural similarity between LDT-611 and its structural analogs selected with Tanimoto coefficient > 0.78. (PNG)

S2 Fig. Activity of chloroquine on *P. berghei* (ookluc) gamete fertilization and consequent ookinete formation on conversion assay. Luciferase activity (light emission in relative light units) is expressed as means ± SEM and is directly proportional to gamete fertilization and ookinete conversion. (N = 2–3).
(PNG)

S3 Fig. Resistome assay establishes no cross-resistance between LDT-623 and major drug targets and mechanisms of antimalarial resistance. (A) Cumulative growth profiles for LDT-623 (4-AQ), a known PI4-kinase inhibitor KDU691, and an untreated control. Drug pressure of 3 x IC_{50} was maintained constant for 14 days and the pool exhibited no growth recovery for LDT-623, whereas recrudescence was observed after 7 days with KDU691. **(B)** Barcode profiles (days 0 and 14) for the no-drug control and the recovered parasites treated with KDU691. Cultures treated with KDU691 showed enrichment of PI4-kinase mutant parasites. Cultures were run in triplicate.
(JPG)

S1 Table. Data supporting the multistage antiplasmodial activity of LDT-623 (*P. falciparum* stage VI-V gametocytes, *P. berghei* ookinetes, and *P. berghei* liver schizonts).
(XLSX)

S2 Table. Absolute values of heme species (Hb, Heme, Hz) identified upon heme fractionation profiling of LDT-623, chloroquine, and KAE609.
(XLSX)

S3 Table. Data on transport assays using PfCRT-containing proteoliposomes.
(XLSX)

S4 Table. Antimalarial IC_{50} and IC_{90} values of LDT-623 tested in *pfcrt*-edited parasite lines.
(XLSX)

S5 Table. Antimalarial IC_{50} and IC_{90} values of LDT-623 tested in *pfmdr1*-modified parasite lines.
(XLSX)

S6 Table. *In vitro* survival curves of *P. falciparum* populations after LDT-623 resistance selection.
(XLSX)

S7 Table. Starting composition (% proportion on day 0) of each barcoded line for the resistome assay. Strain background (3D7 or Dd2), gene name and ID, mutation, and input % are indicated. Growth of parasite pool is shown in S3 Fig.
(XLSX)

Author Contributions

Conceptualization: Letícia Tiburcio Ferreira, Gustavo Capatti Cassiano, David A. Fidock, Fabio Trindade Maranhão Costa.

Data curation: Letícia Tiburcio Ferreira.

Formal analysis: Letícia Tiburcio Ferreira, Gustavo Capatti Cassiano, Luis Carlos Salazar Alvarez, John Okombo, Juliana Calit, Diana Fontinha, Eva Gil-Iturbe, Rachael Coyle.

References

1. World Health Organization. World Malaria Report 2023. 2023.

2. Ariey F, Witkowski B, Amaratunga C, Beghain J, Langlois A-C, Khim N, et al. A molecular marker of artemisinin-resistant *Plasmodium falciparum* malaria. Nature. 2014; 57: 742–68. https://doi.org/10.1038/nature12876 PMID: 24352242

3. van der Pluijm RW, Imwong M, Chau NH, Hoa NT, Thuy-Nhien NT, Thanh NV, et al. Determinants of dihydroartemisinin-piperaquine treatment failure in *Plasmodium falciparum* malaria in Cambodia, Thailand, and Vietnam: a prospective clinical, pharmacological, and genetic study. Lancet Infect Dis. 2019; 19: 952–61. https://doi.org/10.1016/S1473-3099(19)30391-3 PMID: 31345710

4. Imwong M, Dhorda M, Myo Tun K, Thu AM, Phyo AP, Proux S, et al. Molecular epidemiology of resistance to antimalarial drugs in the Greater Mekong subregion: an observational study. Lancet Infect Dis. 2020; 20: 1470–80. https://doi.org/10.1016/S1473-3099(20)30228-0 PMID: 32679084

5. Conrad MD, Asua V, Garg S, Giesbrecht D, Niaré K, Smith S, et al. Evolution of partial resistance to artemisinins in malaria parasites in Uganda. N Engl J Med. 2023; 389: 722–32. https://doi.org/10.1056/NEJMoa2211803 PMID: 37611122

6. Fola AA, Feleke SM, Mohammed H, Brhane BG, Hennelly CM, Assefa A, et al. *Plasmodium falciparum* resistant to artemisinin and diagnostics have emerged in Ethiopia. Nat Microbiol. 2023 8:10. 2023;8: 1911–9. https://doi.org/10.1038/s41564-023-01461-4 PMID: 37640962

7. Mihreteab S, Platon L, Berhane A, Stokes BH, Warsame M, Campagne P, et al. Increasing prevalence of artemisinin-resistant HRP2-negative malaria in Eritrea. N Engl J Med. 2023; 389: 1191–202. https://doi.org/10.1056/NEJMoa2210956 PMID: 37754284

8. Phyo AP, Nkhoma S, Stepniewska K, Ashley EA, Nair S, McGready R, et al. Emergence of artemisinin-resistant malaria on the western border of Thailand: a longitudinal study. The Lancet. 2012; 379: 1960–1966. https://doi.org/10.1016/S0140-6736(12)60484-X PMID: 22484134

9. Flegg JA, Guerin PJ, White NJ, Stepniewska K. Standardizing the measurement of parasite clearance in falciparum malaria: the parasite clearance estimator. Malar J. 2011; 10: 339. https://doi.org/10.1186/1475-2875-10-339 PMID: 22074219

10. Dondorp AM, François N, Poravuth Y, Debashish D, Phae PA, Joel T, et al. Artemisinin resistance in *Plasmodium falciparum* malaria. N Engl J Med. 2009; 361: 455–67. https://doi.org/10.1056/NEJMoa0808859 PMID: 19641202

11. Witkowski B, Amaratunga C, Khim N, Sreng S, Chim P, Kim S, et al. Novel phenotypic assays for the detection of artemisinin-resistant *Plasmodium falciparum* malaria in Cambodia: *in-vitro* and *ex-vivo* drug-response studies. Lancet Infect Dis. 2013; 13: 1043–9. https://doi.org/10.1016/S1473-3099(13)70252-4 PMID: 24035558.

12. Kumar S, Guha M, Choubey V, Maity P, Bandyopadhyay U. Antimalarial drugs inhibiting hemozoin (β-hematin) formation: A mechanistic update. Life Sci. 2007; 80: 813–28. https://doi.org/10.1016/j.lfs.2006.11.008 PMID: 17157328

13. de Villiers KA, Egan TJ. Heme Detoxification in the malaria parasite: a target for antimalarial drug development. Acc Chem Res. 2021; 54: 2649–59. https://doi.org/10.1021/acs.accounts.1c00154 PMID: 33982570

14. Kaschula CH, Egan TJ, Hunter R, Basilico N, Parapini S, Taramelli D, et al. Structure-activity relationships in 4-aminoquinoline antiplasmodials. The role of the group at the 7-position. J Med Chem. 2002; 45: 3531–9. https://doi.org/10.1021/jm020858u PMID: 12139464

15. Egan TJ, Hunter R, Kaschula CH, Marques HM, Misplon A, Walden J. Structure-function relationships in aminoquinolines: Effect of amino and chloro groups on quinoline-hematin complex formation, inhibition of β- hematin formation, and antiplasmodial activity. J Med Chem. 2000; 43: 283–91. https://doi.org/10.1021/jm990437l PMID: 10649984

16. Wicht KJ, Mok S, Fidock DA. Molecular mechanisms of drug resistance in *Plasmodium falciparum* malaria. Annu Rev Microbiol. 2020; 74: 431–54. https://doi.org/10.1146/annurev-micro-020518-115546 PMID: 32905757

17. Sanchez CP, Manson EDT, Cubel SM, Mandel L, Weidt SK, Barrett MP, et al. The knock-down of the chloroquine resistance transporter PfCRT is linked to oligopeptide handling in *Plasmodium falciparum*. Microbiol Spectr. 2022; 10: e0110122. https://doi.org/10.1128/spectrum.01101-22 PMID: 35867395

18. Fidock D, Nomura T, Talley AK, Cooper RA, Dzekunov SM, Ferdig MT, et al. Mutations in the *P. falciparum* digestive vacuole transmembrane protein PfCRT and evidence for their role in chloroquine resistance. Mol Cell. 2000; 6: 861–71. https://doi.org/10.1016/s1097-2765(05)00077-8 PMID: 11090624

19. Ross LS, Dhingra SK, Mok S, Yeo T, Wicht KJ, Kümpornsin K, et al. Emerging Southeast Asian PfCRT mutations confer *Plasmodium falciparum* resistance to the first-line antimalarial piperaquine. Nat Commun 2018; 9: 3314. https://doi.org/10.1038/s41467-018-05652-0 PMID: 30115924

20. Kim J, Tan YZ, Wicht KJ, Erramilli SK, Dhingra SK, Okombo J, et al. Structure and drug resistance of the *Plasmodium falciparum* transporter PfCRT. Nature. 2019; 576: 315–20. https://doi.org/10.1038/s41586-019-1795-x PMID: 31776516

21. Hrycyna CA, Summers RL, Lehane AM, Pires MM, Namanja H, Bohn K, et al. Quinine dimers are potent inhibitors of the *Plasmodium falciparum* chloroquine resistance transporter and are active against quinoline-resistant *P. falciparum*. ACS Chem Biol. 2014; 9: 722–30. https://doi.org/10.1021/cb4008953 PMID: 24369685

22. Ravindar L, Hasbullah SA, Rakesh KP, Hassan NI. Recent developments in antimalarial activities of 4-aminoquinoline derivatives. Eur J Med Chem. 2023; 256: 115458. https://doi.org/10.1016/j.ejmech.2023.115458 PMID: 37163950

23. Ferreira LT, Borba JVB, Moreira-Filho JT, Rimoldi A, Andrade CH, Costa FTM. QSAR-based virtual screening of natural products database for identification of potent antimalarial hits. Biomolecules. 2021; 11: 459. https://doi.org/10.3390/biom11030459 PMID: 33808643

24. Lambros C, Vanderberg JP. Synchronization of *Plasmodium falciparum* erythrocytic stages in culture. J Parasitol. 1979; 65: 418–20. PMID: 383936.

25. Mosmann T. Rapid colorimetric assay for cellular growth and survival: application to proliferation and cytotoxicity assays. J Immunol Methods. 1983; 65: 55–63. https://doi.org/10.1016/0022-1759(83)90303-4 PMID: 6606682.

26. Vaughan AM, Mikolajczak SA, Camargo N, Lakshmanan V, Kennedy M, Lindner SE, et al. A transgenic *Plasmodium falciparum* NF54 strain that expresses GFP-luciferase throughout the parasite life cycle. Mol Biochem Parasitol. 2012; 186: 143–7. https://doi.org/10.1016/j.molbiopara.2012.10.004 PMID: 23107927

27. Fivelman QL, McRobert L, Sharp S, Taylor CJ, Saeed M, Swales CA, et al. Improved synchronous production of *Plasmodium falciparum* gametocytes *in vitro*. Mol Biochem Parasitol. 2007; 154: 119–23. https://doi.org/10.1016/j.molbiopara.2007.04.008 PMID: 17521751

28. Swann J, Corey V, Scherer CA, Kato N, Comer E, Maetani M, et al. High-throughput luciferase-based assay for the discovery of therapeutics that prevent malaria. ACS Infect Dis. 2016; 2: 281–93. https://doi.org/10.1021/acsinfecdis.5b00143 PMID: 27275010

29. Calit J, Drobescu I, Gaitán XA, Borges MH, Ramos MS, Eastman RT, et al. Screening the Pathogen Box against *Plasmodium* sexual stages using a new nanoluciferase based transgenic line of *P. berghei* identifies transmission-blocking compounds. Antimicrob Agents Chemother. 2018; 62: e1053–18. https://doi.org/10.1128/AAC.01053-18 PMID: 30181368

30. Yuda M, Sawai T, Chinzei Y. Structure and expression of an adhesive protein–like molecule of mosquito invasive-stage malarial parasite. J Exp Med. 1999; 189: 1947–52. https://doi.org/10.1084/jem.189.12.1947 PMID: 10377190

31. Ploemen IHJ, Prudêncio M, Douradinha BG, Ramesar J, Fonager J, Van Gemert GJ, et al. Visualization and quantitative analysis of the rodent malaria liver stage by real-time imaging. PLoS One. 2009; 4: 1–12. https://doi.org/10.1371/journal.pone.0007881 PMID: 19924309

32. Bazzone A, Barthmes M. Functional characterization of SLC transporters using solid supported membranes. In: Postis VLG, Goldman A, editors. Biophysics of membrane proteins: methods and protocols. New York, NY: Springer US; 2020. pp. 73–103.

33. Weng J, Zhou X, Wiriyasermkul P, Ren Z, Chen K, Gil-Iturbe E, et al. Insight into the mechanism of H+-coupled nucleobase transport. Proc Natl Acad Sci USA. 2023; 120: e2302799120. https://doi.org/10.1073/pnas.2302799120 PMID: 37549264

34. Szabo G, Eisenman G, Laprade R, Ciani SM, Krasne S. Experimentally observed effects of carriers on the electrical properties of bilayer membranes—equilibrium domain. With a contribution on the molecular basis of ion selectivity. Membranes. 1973; 2: 179–328. PMID: 4585227.

35. Jung H, Tebbe S, Schmid R, Jung K. Unidirectional reconstitution and characterization of purified Na+/proline transporter of *Escherichia coli*. Biochemistry. 1998; 37: 11083–8. https://doi.org/10.1021/bi980684b PMID: 9693004

36. Combrinck JM, Fong KY, Gibhard L, Smith PJ, Wright DW, Egan TJ. Optimization of a multi-well colorimetric assay to determine haem species in *Plasmodium falciparum* in the presence of anti-malarials. Malar J. 2015; 14: 253. https://doi.org/10.1186/s12936-015-0729-9 PMID: 26099266

37. Ng CL, Fidock DA. *Plasmodium falciparum in vitro* drug resistance selections and gene editing. Methods Mol Biol. 2019; 2013: 123–40. https://doi.org/10.1007/978-1-4939-9550-9_9 PMID: 31267498

38. Kümpornsin K, Kochakarn T, Yeo T, Okombo J, Luth MR, Hoshizaki J, et al. Generation of a mutator parasite to drive resistome discovery in *Plasmodium falciparum*. Nat Commun. 2023; 14: 3059. https://doi.org/10.1038/s41467-023-38774-1 PMID: 37244916

39. Istvan ES, Mallari JP, Corey VC, Dharia N V., Marshall GR, Winzeler EA, et al. Esterase mutation is a mechanism of resistance to antimalarial compounds. Nat Commun. 2017; 8: 14240. https://doi.org/10.1038/ncomms14240 PMID: 28106035

40. Carrasquilla M, Drammeh NF, Rawat M, Sanderson T, Zenonos Z, Rayner JC, et al. Barcoding genetically distinct *Plasmodium falciparum* strains for comparative assessment of fitness and antimalarial drug resistance. mBio. 2022; 13. https://doi.org/10.1128/MBIO.00937-22 PMID: 35972144

41. Plouffe DM, Wree M, Du AY, Meister S, Li F, Patra K, et al. High-throughput assay and discovery of small molecules that interrupt malaria transmission. Cell Host Microbe. 2016; 19: 114–26. https://doi.org/10.1016/j.chom.2015.12.001 PMID: 26749441

42. Bouzón-Arnáiz I, Avalos-Padilla Y, Biosca A, Caño-Prades O, Román-Álamo L, Valle J, et al. The protein aggregation inhibitor YAT2150 has potent antimalarial activity in *Plasmodium falciparum in vitro* cultures. BMC Biol. 2022; 20: 1–27. https://doi.org/10.1186/s12915-022-01374-4 PMID: 36271358

43. Fong KY, Wright DW. Hemozoin and antimalarial drug discovery. Future Med Chem. 2013; 5: 1437–50. https://doi.org/10.4155/fmc.13.113 PMID: 23919553

44. Sullivan DJ. Quinolines block every step of malaria heme crystal growth. Proc Natl Acad Sci USA. 2017; 114: 7483–5. https://doi.org/10.1073/pnas.1708153114 PMID: 28696317

45. Spillman NJ, Allen RJW, McNamara CW, Yeung BKS, Winzeler EA, Diagana TT, et al. Na+ regulation in the malaria parasite *Plasmodium falciparum* involves the cation ATPase PfATP4 and is a target of the spiroindolone antimalarials. Cell Host Microbe. 2013; 13: 227–37. https://doi.org/10.1016/j.chom.2012.12.006 PMID: 23414762

46. Riegel B, Roepe PD. Altered drug transport by *Plasmodium falciparum* chloroquine resistance transporter isoforms harboring mutations associated with piperaquine resistance. Biochemistry. 2020; 59: 2484–93. https://doi.org/10.1021/acs.biochem.0c00247 PMID: 32589406

47. Pelleau S, Moss EL, Dhingra SK, Volney B, Casteras J, Gabryszewski SJ, et al. Adaptive evolution of malaria parasites in French Guiana: Reversal of chloroquine resistance by acquisition of a mutation in

pfcrt. Proc Natl Acad Sci USA. 2015; 112: 11672–7. https://doi.org/10.1073/pnas.1507142112 PMID: 26261345

48. Birth D, Kao WC, Hunte C. Structural analysis of atovaquone-inhibited cytochrome bc1 complex reveals the molecular basis of antimalarial drug action. Nat Commun. 2014; 5: 4029. https://doi.org/10.1038/ncomms5029 PMID: 24893593

49. Walter RD. Altered dihydrofolate reductase in pyrimethamine-resistant *Plasmodium falciparum*. Mol Biochem Parasitol. 1986; 19: 61–6. https://doi.org/10.1016/0166-6851(86)90066-6 PMID: 3520313

50. Assur Sanghai Z, Liu Q, Clarke OB, Belcher-Dufrisne M, Wiriyasermkul P, Giese MH, et al. Structure-based analysis of CysZ-mediated cellular uptake of sulfate. eLife. 2018; 7: e27829. https://doi.org/10.7554/eLife.27829 PMID: 29792261

51. Small-Saunders JL, Hagenah LM, Wicht KJ, Dhingra SK, Deni I, Kim J, et al. Evidence for the early emergence of piperaquine-resistant *Plasmodium falciparum* malaria and modeling strategies to mitigate resistance. PLoS Pathog. 2022; 18: e1010278. https://doi.org/10.1371/journal.ppat.1010278 PMID: 35130315

52. Dhingra SK, Small-Saunders JL, Ménard D, Fidock DA. *Plasmodium falciparum* resistance to piperaquine driven by PfCRT. Lancet Infect Dis. 2019; 19: 1168–9. https://doi.org/10.1016/S1473-3099(19)30543-2 PMID: 31657776

53. Dhingra SK, Gabryszewski SJ, Small-Saunders JL, Yeo T, Henrich PP, Mok S, et al. Global spread of mutant PfCRT and its pleiotropic impact on *Plasmodium falciparum* multidrug resistance and fitness. mBio. 2019; 10: e02731–18. https://doi.org/10.1128/mBio.02731-18 PMID: 31040246

54. Sidhu ABS, Uhlemann AC, Valderramos SG, Valderramos JC, Krishna S, Fidock DA. Decreasing *pfmdr1* copy number in *Plasmodium falciparum* malaria heightens susceptibility to mefloquine, lumefantrine, halofantrine, quinine, and artemisinin. J Infect Dis. 2006; 194: 528–35. https://doi.org/10.1086/507115 PMID: 16845638

55. Veiga MI, Dhingra SK, Henrich PP, Straimer J, Gnädig N, Uhlemann AC, et al. Globally prevalent PfMDR1 mutations modulate *Plasmodium falciparum* susceptibility to artemisinin-based combination therapies. Nat Commun. 2016; 7: 11553. https://doi.org/10.1038/ncomms11553 PMID: 27189525

56. Happi CT, Gbotosho GO, Folarin OA, Sowunmi A, Bolaji OM, Fateye BA, et al. Linkage disequilibrium between two distinct loci in chromosomes 5 and 7 of *Plasmodium falciparum* and *in vivo* chloroquine resistance in Southwest Nigeria. Parasitol Res. 2006; 100: 141–8. https://doi.org/10.1007/s00436-006-0246-4 PMID: 16874478

57. Sá JM, Twu O, Hayton K, Reyes S, Fay MP, Ringwald P, et al. Geographic patterns of *Plasmodium falciparum* drug resistance distinguished by differential responses to amodiaquine and chloroquine. Proc Natl Acad Sci USA. 2009; 106: 18883–9. https://doi.org/10.1073/pnas.0911317106 PMID: 19884511

58. Bopp S, Magistrado P, Wong W, Schaffner SF, Mukherjee A, Lim P, et al. Plasmepsin II–III copy number accounts for bimodal piperaquine resistance among Cambodian *Plasmodium falciparum*. Nat Commun. 2018 9: 1769. https://doi.org/10.1038/s41467-018-04104-z PMID: 29720620

59. Spyropoulos IC, Liakopoulos TD, Bagos PG, Hamodrakas SJ. TMRPres2D: high quality visual representation of transmembrane protein models. Bioinformatics. 2004; 20: 3258–60. https://doi.org/10.1093/bioinformatics/bth358 PMID: 15201184

60. Corey VC, Lukens AK, Istvan ES, Lee MCS, Franco V, Magistrado P, et al. A broad analysis of resistance development in the malaria parasite. Nat Commun. 2016; 7: 11901. https://doi.org/10.1038/ncomms11901 PMID: 27301419

61. Cowell AN, Istvan ES, Lukens AK, Gomez-Lorenzo MG, Vanaerschot M, Sakata-Kato T, et al. Mapping the malaria parasite druggable genome by using *in vitro* evolution and chemogenomics. Science 2018; 359: 191–9. https://doi.org/10.1126/science.aan4472 PMID: 29326268

62. Forte B, Ottilie S, Plater A, Campo B, Dechering KJ, Gamo FJ, et al. Prioritization of molecular targets for antimalarial drug discovery. ACS Infect Dis. 2021; 7: 2764–76. https://doi.org/10.1021/acsinfecdis.1c00322 PMID: 34523908

63. McNamara CW, Lee MC, Lim CS, Lim SH, Roland J, Simon O, et al. Targeting *Plasmodium* PI(4)K to eliminate malaria. Nature. 2013; 504: 248–53. https://doi.org/10.1038/nature12782 PMID: 24284631

64. Baragaña B, Hallyburton I, Lee MCS, Norcross NR, Grimaldi R, Otto TD, et al. A novel multiple-stage antimalarial agent that inhibits protein synthesis. Nature. 2015; 522: 315–20. https://doi.org/10.1038/nature14451 PMID: 26085270

65. Gamo FJ, Sanz LM, Vidal J, De Cozar C, Alvarez E, Lavandera JL, et al. Thousands of chemical starting points for antimalarial lead identification. Nature. 2010; 465: 305–10. https://doi.org/10.1038/nature09107 PMID: 20485427

66. Mathieu LC, Cox H, Early AM, Mok S, Lazrek Y, Paquet JC, et al. Local emergence in Amazonia of *Plasmodium falciparum* K13 C580Y mutants associated with *in vitro* artemisinin resistance. eLife. 2020; 9: 1–21. https://doi.org/10.7554/eLife.51015 PMID: 32394893

67. Florimond C, de Laval F, Early AM, Sauthier S, Lazrek Y, Pelleau S, et al. Impact of piperaquine resistance in *Plasmodium falciparum* on malaria treatment effectiveness in The Guianas: a descriptive epidemiological study. Lancet Infect Dis. 2024; 24: 161–71. https://doi.org/10.1016/S1473-3099(23)00502-9 PMID: 37858325

68. Parobek CM, Parr JB, Brazeau NF, Lon C, Chaorattanakawee S, Gosi P, et al. Partner-drug resistance and population substructuring of artemisinin-resistant *Plasmodium falciparum* in Cambodia. Genome Biol Evol. 2017; 9: 1673–86. https://doi.org/10.1093/gbe/evx126 PMID: 28854635

69. Leang R, Taylor WRJ, Bouth DM, Song L, Tarning J, Char MC, et al. Evidence of *Plasmodium falciparum* malaria multidrug resistance to artemisinin and piperaquine in western Cambodia: dihydroartemisinin-piperaquine open-label multicenter clinical assessment. Antimicrob Agents Chemother. 2015; 59: 4719–26. https://doi.org/10.1128/AAC.00835-15 PMID: 26014949

70. Sisowath C, Petersen I, Veiga MI, Mårtensson A, Premji Z, Björkman A, et al. *In vivo* selection of *Plasmodium falciparum* parasites carrying the chloroquine-susceptible *pfcrt* K76 allele after treatment with artemether-lumefantrine in Africa. J Infect Dis. 2009; 199: 750–7. https://doi.org/10.1086/596738 PMID: 19210165

71. Conrad MD, LeClair N, Arinaitwe E, Wanzira H, Kakuru A, Bigira V, et al. Comparative impacts over 5 years of artemisinin-based combination therapies on *Plasmodium falciparum* polymorphisms that modulate drug sensitivity in Ugandan children. J Infect Dis. 2014; 210: 344–53. https://doi.org/10.1093/infdis/jiu141 PMID: 24610872

72. Venkatesan M, Gadalla NB, Stepniewska K, Dahal P, Nsanzabana C, Moriera C, et al. Polymorphisms in *Plasmodium falciparum* chloroquine resistance transporter and multidrug resistance 1 genes: parasite risk factors that affect treatment outcomes for *P. falciparum* malaria after artemether-lumefantrine and artesunate-amodiaquine. Am J Trop Med Hyg. 2014; 91: 833–43. https://doi.org/10.4269/ajtmh.14-0031 PMID: 25048375

73. Cheeseman IH, Miller B, Tan JC, Tan A, Nair S, Nkhoma SC, et al. Population structure shapes copy number variation in malaria parasites. Mol Biol Evol. 2016; 33: 603–20. https://doi.org/10.1093/molbev/msv282 PMID: 26613787

74. Yoo E, Schulze CJ, Stokes BH, Onguka O, Yeo T, Mok S, et al. The antimalarial natural product Salinipostin A identifies essential α/β serine hydrolases involved in lipid metabolism in *P. falciparum* parasites. Cell Chem Biol. 2020; 27: 143–57. https://doi.org/10.1016/j.chembiol.2020.01.001 PMID: 31978322

75. Le Manach C, Paquet T, Wicht K, Nchinda AT, Brunschwig C, Njoroge M, et al. Antimalarial lead-optimization studies on a 2,6-imidazopyridine series within a constrained chemical space to circumvent atypical dose-response curves against multidrug-resistant parasite strains. J Med Chem. 2018; 61: 9371–85. https://doi.org/10.1021/acs.jmedchem.8b01333 PMID: 30256636

76. Patel V, Booker M, Kramer M, Ross L, Celatka CA, Kennedy LM, et al. Identification and characterization of small molecule inhibitors of *Plasmodium falciparum* dihydroorotate dehydrogenase. J Biol Chem. 2008; 283: 35078–85. https://doi.org/10.1074/jbc.M804990200 PMID: 18842591

77. Blasco B, Leroy D, Fidock DA. Antimalarial drug resistance: linking *Plasmodium falciparum* parasite biology to the clinic. Nat Med. 2017; 23: 917–28. https://doi.org/10.1038/nm.4381 PMID: 28777791

78. McCarthy JS, Rückle T, Djeriou E, Cantalloube C, Ter-Minassian D, Baker M, et al. A Phase II pilot trial to evaluate safety and efficacy of ferroquine against early *Plasmodium falciparum* in an induced blood-stage malaria infection study. Malar J. 2016; 15: 469. https://doi.org/10.1186/s12936-016-1511-3 PMID: 27624471

79. Held J, Supan C, Salazar CLO, Tinto H, Bonkian LN, Nahum A, et al. Ferroquine and artesunate in African adults and children with *Plasmodium falciparum* malaria: a phase 2, multicentre, randomised, double-blind, dose-ranging, non-inferiority study. Lancet Infect Dis. 2015; 15: 1409–19. https://doi.org/10.1016/S1473-3099(15)00079-1 PMID: 26342427

80. Wells TN, H van Huijsduijnen R. Ferroquine: welcome to the next generation of antimalarials. Lancet Infect Dis. 2015; 15: 1365–6. https://doi.org/10.1016/S1473-3099(15)00148-6 PMID: 26342426

81. Gansane A, Lingani M, Yeka A, Nahum A, Bouyou-Akotet M, Mombo-Ngoma G, et al. Randomized, open-label, phase 2a study to evaluate the contribution of artefenomel to the clinical and parasiticidal activity of artefenomel plus ferroquine in African patients with uncomplicated *Plasmodium falciparum* malaria. Malar J. 2023; 22: 1–16. https://doi.org/10.1186/s12936-022-04420-2 PMID: 36597076

82. Beshir K, Sutherland CJ, Merinopoulos I, Durrani N, Leslie T, Rowland M, et al. Amodiaquine resistance in *Plasmodium falciparum* malaria in Afghanistan is associated with the *pfcrt* SVMNT allele at codons 72 to 76. Antimicrob Agents Chemother. 2010; 54: 3714–6. https://doi.org/10.1128/AAC.00358-10 PMID: 20547800

83. Kelly JX, Smilkstein MJ, Brun R, Wittlin S, Cooper RA, Lane KD, et al. Discovery of dual function acridones as a new antimalarial chemotype. Nature. 2009; 459: 270–3. https://doi.org/10.1038/nature07937 PMID: 19357645

84. Gunsaru B, Burgess SJ, Morrill W, Kelly JX, Shomloo S, Smilkstein MJ, et al. Simplified reversed chloroquines to overcome malaria resistance to quinoline-based drugs. Antimicrob Agents Chemother. 2017; 61: e01913–16. https://doi.org/10.1128/AAC.01913-16 PMID: 28193646